

FREE CONVECTION HEAT TRANSFER FROM
A HORIZONTAL PLATE FACING DOWNWARDS

FREE CONVECTION HEAT TRANSFER FROM
A HEATED HORIZONTAL PLATE FACING DOWNWARDS

By

SHIAM SUNDER GUPTA, B. TECH.

A Thesis

Submitted To The Faculty Of Graduate Studies

In Partial Fulfilment Of The Requirements

For The Degree

Master Of Engineering

McMaster University

November, 1968

MASTER OF ENGINEERING (1968)
(Mechanical Engineering)

McMASTER UNIVERSITY
Hamilton, Ontario

TITLE: FREE CONVECTION HEAT TRANSFER FROM A HEATED
HORIZONTAL PLATE FACING DOWNWARDS

AUTHOR: SHIAM SUNDER GUPTA, B. Tech. (Indian Institute of
Technology, Kanpur, India)

SUPERVISOR: Dr. R. L. JUDD

NUMBER OF PAGES: (v), 70

SCOPE AND CONTENTS:

An experimental study of free convection heat transfer from a heated horizontal plate facing downwards in air is reported in this thesis. The results of this study are in good agreement with the results obtained by Fishenden and Saunders. This study also investigates the effect of restraining the development of the thermal boundary layer with 1/2" and 1" edge strips around the edges of the test plate. This study led to the conclusion that edge restraints tended to decrease the heat transfer from the plate.

The range of Grashof Prandtl Number product investigated is between 4×10^8 and 8×10^9 resulting in the heat flux range of 0.7 Btu/hrft² to 102 Btu/hrft². Correlations are presented relating heat flux and temperature difference between plate surface temperature and ambient temperature.

ACKNOWLEDGEMENTS

The author gratefully acknowledges the assistance and support of Doctor R. L. Judd who provided guidance and advice in planning and performing of this experimental study.

The financial support provided by National Research Council Grant A 4362 is gratefully acknowledged.

TABLE OF CONTENTS

TEXT	PAGE
1. Introduction	1
2. Literature Survey	3
3. Test Facility	7
3.1 Test Equipment	7
3.2 Instrumentation	9
3.3 Qualitative Measurement Of The Thermal Boundary Layer Below The Plate	13
4. Test Conditions	14
4.1 Plate Temperature	14
4.2 Grashof Prandtl Number Product	14
4.3 Edge Restraints	15
5. Data Reduction	16
6. Results	20
7. Discussion	24
7.1 Accuracy of Results	24
7.2 Heat Flux Correlation	27
7.3 Effect of Edge Restraints	28
7.4 Nusselt Number Correlation	29
7.5 Air Temperature Fluctuations	30
8. Conclusions	32
9. References	33
10. Illustrations	34
Figure 1 - Test Facility Front View	35
Figure 2 - Test Facility Side View	37

	PAGE
Figure 3 - Test Plate	39
Figure 4 - Heater Wiring Diagram	40
Figure 5 - Thermocouple Wiring Diagram	41
Figure 6 - Thermocouple Probe	42
Figure 7 - Thermocouple Probe With Stand And Other Accessories.....	44
Figure 8 - Plot of Gr x Pr Vs. ΔT	46
Figure 9 - Arrangement Of Edge Strips Or Fins	47
Figure 10 - Temperature Recording Samples No Fin Configuration	48
Figure 11 - Temperature Recording Samples 1/2" Fin Configuration	49
Figure 12 - Temperature Recording Samples 1" Fin Configuration	50
Figure 13 - Temperature Profiles, Highest ΔT Level, No Fin Configuration	51
Figure 14 - Temperature Profiles, Lower ΔT Levels, No Fin Configuration	52
Figure 15 - Temperature Profiles, Highest ΔT Level, 1/2" Fin Configuration	53
Figure 16 - Temperature Profiles, Lower ΔT Levels, 1/2" Fin Configuration.....	54
Figure 17 - Temperature Profiles, Highest ΔT Level, 1" Fin Configuration	55
Figure 18 - Temperature Profiles, Lower ΔT Levels, 1" Fin Configuration	56
Figure 19 - Plot Of Q/A Vs. ΔT Uniform Heat Flux Assumption	57
Figure 20 - Plot Of Q/A Vs. ΔT Discrete Heat Flux Assumption	58

	PAGE
Figure 21 - Temperature Profiles At Centre, Side And Corner	59
Figure 22 - Schlieren Photograph Of Thermal Boundary Layer Near Centre	60
Figure 23 - Schlieren Photograph Of Thermal Boundary Layer Near Edges	60
Figure 24 - Fishenden And Saunders Correlation..	61
Figure 25 - Comparison With Fishenden And Saunders Relationship, Calculations Based On Uniform Heat Flux Assumption	62
Figure 26 - Comparison With Fishenden And Saunders Relationship, Calculations Based On Discrete Heat Flux Assumption	62
Figure 27 - Envelope Of Fluctuations About Time Averaged Curve	63
Figure 28 - Temperature Profiles Obtained With Various Probes	65

APPENDIX

A Probe Design	64
B Energy Balance	66

TEXT

1. INTRODUCTION

This dissertation concerns the experimental study of heat transfer to still air from a heated horizontal plate facing downward. The study was prompted by the fact that very little information was available for this configuration, and that the published experimental results were not sufficient to enable one to draw a firm conclusion, since all major heat transfer books indicated only one reference.

Moreover, no mention had been made by any of the investigators regarding the effect on heat transfer behaviour caused by restraining the flow of hot air from below the horizontal plate. For the present experimental study, this flow restraint was achieved by attaching strips all around the edges and perpendicular to the horizontal surface of the test plate. Three sets of measurements were taken with 0", 0.5" and 1" wide edge strips respectively. Such information could be useful in the design of industrial or experimental heat transfer systems.

Correlations are presented relating the Nusselt number to the Grashof Prandtl number product and relating the heat flux, the amount of heat transferred per unit area per unit time, directly to the difference between plate temperature and ambient temperature as a first hand approximation.

The range of Grashof Prandtl number product investigated was between 4×10^8 to 8×10^9 for the temperature difference range between 5°F to 225°F . Within this range of temperature difference, five tests were performed for each of the edge constraint configuration mentioned before, at five levels of temperature difference chosen on the basis of even intervals on a logarithmic scale.

By similarity, it may be seen that the process of heat loss by natural convection from a heated horizontal plane surface facing downwards, is akin to that of heat gain by a similar cooled surface facing upwards, for the same temperature difference and the same film temperature. The results of the present study for a hot surface facing downwards, therefore, can be used for the heat transfer to a cool surface facing upwards.

2. LITERATURE SURVEY

Brown and Marco (1) performed a dimensional analysis of the various parameters affecting free convection using the π theorem which led to an equation of the form

$$\frac{h_c \ell}{k} = \alpha \left(\frac{g \beta \Delta T \ell^3 \rho^2}{\mu^2} \right)^\beta \left(\frac{C_p \mu}{k} \right)^\gamma \quad (1)$$

where $\frac{g \beta \Delta T \ell^3 \rho^2}{\mu^2}$ is the Grashof Number Gr.

and $\frac{C_p \mu}{k}$ is the Prandtl Number Pr.

Brown and Marco further indicated that the results of a number of tests investigating free convection to various fluids both liquids and gases from different surface configurations showed that β and γ were numerically the same. Hence Equation (1) reduced to

$$\frac{h_c \ell}{k} = c (Gr Pr)^d \quad (2)$$

Brown and Marco also stated that horizontal plates with the warm side facing upwards transferred twice as much heat per degree of temperature difference as did similar plates with the warm side facing downward. For $10^3 < GrPr < 10^9$ the relationship recommended was

$$\frac{h_c \ell}{k} = c(GrPr)^{1/4} \quad (3)$$

whereas for $GrPr > 10^9$ the relationship

$$\frac{h_c \ell}{k} = c' (GrPr)^{1/3} \quad (4)$$

was recommended which was based upon the experimental work of King (2). Moreover, Brown and Marco stated that the influence of any characteristic dimension greater than 2 feet was negligible in computing the film conductance relating to a surface surrounded by gas. It was implied that the value of characteristic length to be applied in expressions for the film conductance due to free convection should not exceed 2 feet. The values of c and c' recommended for a horizontal plate facing downwards were 0.35 and 0.08 respectively.

Jakob and Linke (3) deduced from their experimental work on horizontal plates facing upward that heat transfer from a horizontal plate was independent of position. In fact, this result is expected because there is no reason why the heat transfer at one position on a horizontal plate should be different from that at any other position except close to the edges. Jakob (4) derived the following equations

$$q''_{h,u} = 0.275 (\Delta T)^{4/3} \quad (5)$$

and

$$q''_{h,d} = 0.5 q''_{h,u} \quad (6)$$

from the experimental work of Griffith and Davis (5) for the heat flux from heated horizontal surfaces facing upwards and downwards

respectively. Quoting from Jakob,

“ Even a smaller factor than 0.50 might be expected because of the fact that there is no reason for any convection when the hot air is above the colder air. Actually, some convection is caused by secondary influences, (such) as temperature differences on the edge of the horizontal plate.”

In addition, Jakob presented some results of Weise (6) pertaining to the determination of the temperature distribution on horizontal plate. Weise used two square aluminum plates about 16 cm. and 24 cm. in side length which were hung horizontally in a wide room and heated electrically. The results of a total 70,000 readings were combined to give patterns of isothermal lines, one of which was reproduced by Jakob in Figure (25.5) of Reference (4). This plot shows that the boundary layer in which the temperature drop was concentrated below the plate was about 1.5 cm. thick in the centre and 1 cm. close to the edge. Jakob also presented a Schlieren photograph of a hot horizontal plate in air at rest obtained from the work of Schmidt (7) which is presented as Figure (27-b) of Reference (4).

Fishenden and Saunders (8) presented the results of their experimental work on heated horizontal plates facing upwards and downwards in the form of the correlations

$$Nu = 0.54 (GrPr)^{1/4} \text{ for } 10^5 < GrPr < 10^8 \quad (7)$$

$$Nu = 0.25 (GrPr)^{1/4} \text{ for } 10^5 < GrPr < 10^9 \quad (8)$$

The maximum size of the plate investigated was 2 feet with temperature differences between surface and ambient air up to 1000°F. Fishenden and Saunders also presented a relationship for heat flux in the form

$$q''_{h,d} = \frac{0.12 (\Delta T)^{1.25}}{(L)^{0.25}} \quad (9)$$

for 10^4 or $10^5 < GrPr < 10^8$ or 10^9 for the case of horizontal plate facing downwards.

McAdams (9) indicated that Equation (8) would better fit Fishenden and Saunders data if the coefficient were 0.27.

Kutateladze and Borishanskii (10) indicated values of c and d as 0.54 and $1/4$ for $5 \times 10^2 < GrPr < 10^7$ and 0.135 and $1/3$ for $GrPr > 2 \times 10^7$ for free convection heat transfer from plane surfaces. It was indicated that the value of the coefficient was increased by 30 percent for a warm surface facing upwards and was decreased by 30 percent for a warm surface facing downwards. Then according to Kutateladze and Borishanskii, the correlations for a horizontal plate facing downwards become

$$Nu = 0.38 (GrPr)^{1/4} \quad (10)$$

$$\text{for } 5 \times 10^2 < GrPr < 10^7$$

and

$$Nu = 0.095 (GrPr)^{1/3} \quad (11)$$

$$\text{for } GrPr > 10^7$$

3. TEST FACILITY

Photographs of the test facility used in performing experimental study are shown in Figures 1 and 2.

The apparatus is described in detail in the following section.

3.1 Test Equipment

The test equipment is described in three sections as follows.

3.1.1 Test Plate

A one inch thick by forty five inch square aluminum plate was used as shown in Figure (3). The edges were bevelled in order to permit the hot air from below the plate to flow smoothly around the edges, thus minimizing the disturbance in the air and maintaining a stream line flow all around as represented in Figure 3(c). The plate was further divided into nine zones separated by rectangular slots in an attempt to minimize transverse conduction so as to direct the flow of heat downward.

Appropriate holes were provided in centre of each zone to hold thermocouples for temperature measurements. Each zone contained two holes, one terminating about 1/4" from top surface of the plate and the other terminating about 1/8" from bottom surface. The details of thermocouple holes are shown in Figure 3(b). The holes were arranged so that the thermocouple junctions would terminate on a line perpendicular to the top surface. This was done so that the temperature

of the plate could be measured at two points with a view to evaluating temperature gradient in the plate. Subsequent experience with the apparatus indicated that this was not possible; the difference in temperature was so small as to be masked by the uncertainty of temperature measurement. Horizontal slots were provided around these holes, to enable the thermocouple leads to be arranged horizontally perpendicular to the heat flux, so as to minimize the error in the thermocouple reading caused by the withdrawal of heat from thermocouple junction by conduction along the thermocouple lead.

3.1.2 Heating Source

Chromalox electric strip heating elements rated at 230 volts and 250 watts were fixed to the upper surface of the test plate in each of the nine zones. Different numbers of heaters were used in different zones; namely four in each of the four corner zones and two in each of the side and centre zones. This arrangement satisfied the requirements for different amounts of heat from each zone in order that the test plate might be maintained isothermal. Power input to various groupings of heaters was regulated in order to achieve this condition. The details are further described under instrumentation.

3.1.3. Stand And Other Accessories

As presented in Figure 2, the plate was hung on a six foot high stand which provided space to work below the plate.

Turn-buckles which were used to support the plate on the stand facilitated the levelling of test plate and minimized the heat losses due to conduction from the plate to the stand.

The plate was insulated on the top surface with a six inch layer of fine vermiculite (plaster aggregate, Zonolite brand) to reduce heat losses in the upward direction to a minimum. The vermiculite was enclosed in a sheet metal cover. Two thermocouples were installed on this cover for use in estimating the heat losses through the insulation.

3.2 Instrumentation

3.2.1 Plate Temperature Control

As already mentioned, different numbers of heaters were put in different zones. For heating purposes, the nine zones into which the test plate was divided were grouped into three regions, namely corners, sides and centre. Heat input to these three regions was controlled through power variacs. Figure (4) shows the manner in which the heaters were wired for regional control. Supply of different amount of power to these regions in response to the temperatures measured with thermocouples in different zones, enabled the achievement of uniform temperature all over the plate.

Appropriate points were also provided on the front panel board for the measurement of voltage, amperage and wattage input to the heaters of each region so that an approximate energy balance

could be performed for the system.

3.2.2 Temperature Measurement

The temperature in each of the zones of the plate was measured with eighteen "Ceramo" type thermocouples with six inch immersion length installed in the slots described previously. The temperature of the cover was measured with two thermocouples installed at the corner and centre respectively. Two similar thermocouples were installed on the upper surface of the test plate for measuring the surface temperature. The response of all these thermocouples was referenced to ice temperature. The ice bath was stirred frequently to maintain uniform temperature for all the thermocouple junctions.

The thermoelectric potentials of all these twenty thermocouples were recorded by a Honeywell, model 15303 830-12-(99)-0-000-012-11-060, elektronik 15, twelve point continuously balancing millivolt recorder.

The output of eight thermocouples in four representative zones (two corners, one side and the centre) as well as the output of the two upper surface thermocouples and the two cover thermocouples were recorded consecutively by the recorder. The outputs of other zonal thermocouples were periodically fed to the recorder to measure the temperature of those zones in order to check the uniformity of temperature over the plate.

Double pole, double throw knife switches were provided which in one position fed the output of the zonal thermocouples to the recorder circuit and in the other position enabled the measurement of differential temperature of the two thermocouples in a zone by feeding the differential output to a Honeywell, model No. 2745, millivolt potentiometer. The wiring diagram is shown in Figure (5).

The rated accuracy of the thermocouples used was $\pm .25\%$ of the temperature measurement. The recorder had an accuracy of $\pm .25\%$.

The temperature distribution in the air below the plate was measured with a thermocouple probe described below.

3.2.3 Thermocouple Probe

Quite a few thermocouple probe configurations had to be tried before a probe which gave acceptable results was found. The main reason for rejecting the probes was the discrepancy of the order of 40 - 50°F, between the temperature of the air at zero displacement as obtained by extrapolation of the temperature distribution plotted from the probe measurements and the temperature of the test plate measured by the embedded thermocouples. The various configurations tried and the results obtained are given in Appendix A. Although the discussion of the thermocouple probes which were not acceptable has no bearing on this presentation, it might be

useful in the design of thermocouple probes for other applications. The lower reading of the unacceptable probes was thought to have been due to local convection currents induced by the presence of the supports acting to decrease the temperature of the air at the thermocouple junction.

The probe used for the present study is shown in Figure (6). The edges of the side supports of the probe (20 gauge stainless steel shim) were sharpened to smooth the air flow. The thermocouple was comprised of chromel-alumel, 40 gauge wire butt welded in a mercury bath which resulted in a .010 inch diameter junction. The thermocouple deviated only $\pm .25\%$ from the measurement of a calibrated thermocouple. The probe was positioned by a traversing attachment having .001" resolution and fixed to a tripod stand with levelling screws as shown in Figure (7). The probe moved perpendicular to the base of the traversing attachment, which was levelled by means of the tripod levelling screws and checked with a spirit bubble level.

The thermoelectric potential of the thermocouple was fed to a Honeywell model SY153 x 18 -(V AH 1) - II-III-157-D Brown Elektronik, single point continuous balancing millivolt recorder. Ice temperature was again used as the reference junction temperature. Accuracy of the recorder was $\pm .25\%$.

3.3 Qualitative Estimate of The Thermal Boundary Layer Below The Plate

The thermal boundary layer below the test plate was studied with a Schlieren apparatus. The Schlieren technique enabled the qualitative analysis of the boundary layer through the influence which density changes had upon the transmission of a collimated beam of light. Figure (2) shows the Schlieren apparatus set up for the present study.

4. TEST CONDITIONS

Steady state temperature levels in the test plate were achieved in approximately eight hours after changes in the powerstat settings. The settings of the powerstats were somewhat arbitrary for the first set of tests and adjustments had to be made until the temperature of the plate varied no more than $\pm 1^\circ\text{F}$ at any two positions on the plate. The test conditions are further described under the following headings.

4.1 Plate Temperature

The maximum temperature of the test plate was approximately 335°F resulting in a maximum temperature difference of about 255°F . The minimum temperature achieved was approximately 80°F resulting in about 5°F temperature difference. Five tests were conducted at different plate temperatures between 335°F and 80°F . For each test, the temperature distribution in the air below the plate was scanned at three positions namely centre, side and corner. The exact locations are shown in Figures (13), (15) & (17). Before each test, the traversing attachment of the probe was properly levelled as described previously.

4.2 Grashof Prandtl Number Products

The range of Grashof Prandtl numbers product achieved was 4×10^8 to 8×10^9 for which the corresponding range of heat flux varied between 0.7 Btu/hr ft^2 to 102 Btu/hr ft^2 . A plot of Grashof Prandtl number product versus temperature difference, Figure (8), illustrates that maximum value of Grashof Prandtl product occurs at

a temperature difference of about 325°F. On either side of this value, Grashof Prandtl number product decreases. Therefore, the behaviour of the air properties which governs free convection from the test plate varies in such a fashion that the maximum achievable Grashof Prandtl number product is 8.6×10^9 . This behaviour indicates that in order to achieve a higher Grashof Prandtl number product, one has to choose larger sizes of surface rather than higher surface temperatures.

4.3 Edge Restraints

Strips of metal were added to constrain the thermal boundary layer. Additional sets of measurements were taken, using a 1/2" wide strip and a 1" wide strip respectively. These strips were fixed to the bevelled edges of the test plate so that the original heat transfer area of the plate was not affected as shown in Figure (9). The gaps between the strips and the plate were filled up with plaster of paris in order to prevent the leakage of hot air. Thus the flow of hot air was totally directed over the edges of the edge strips.

The choice of edge strip widths was based upon the thickness of the thermal boundary layer which developed below the plate without edge restraints. The boundary layer thickness was about seven tenths of an inch and hence two widths namely 0.50" and 1.00" were chosen to partially and totally restrain the boundary layer respectively.

5. DATA REDUCTION

As already mentioned, the thermoelectric potential from the thermocouple probe used to scan the temperature distribution in air below the plate was fed to a single point continuous balancing recorder. Random fluctuations of varying magnitudes, depending on the location of the probe, were observed in the air below the plate as illustrated in Figures (10), (11) & (12) showing samples of recorder paper. This point is further discussed in Chapter 7. An average value of the thermoelectric potential was computed from such temperature recordings over a period of about ten minutes by drawing a line such that the area on both sides were equal as estimated by eye judgement. This value was taken as the reading at that particular location as demonstrated in Figures (10), (11) & (12).

Each scan was taken over the range from about 0.020" to 1.400" from the test plate with enough intermediate measurements to obtain a smooth temperature plot. At 1.400" from the plate, the temperature difference between air below the plate and the ambient temperature reduced to the order of 0°F to 3°F depending on the plate temperature and further measurements were not necessary.

A graph of ΔT , the temperature difference between the air temperature and the ambient temperature versus x , the displacement of the thermocouple junction from the bottom surface of the plate, was plotted for each scan as indicated in Figures (13) to (18). These

graphs enabled the determination of the temperature gradient in the air at zero distance from the test plate from which the local heat flux was computed in the following manner.

The heat flux conducted downwards by the plate was equated to the heat flux received by the air by virtue of conduction in the immediate vicinity of the plate i.e. at zero distance from the plate.

Therefore, we can write:

$$Q/A = - k_a \left. \frac{dT}{dx} \right|_{x=0} \quad (12)$$

where k_a : Thermal conductivity of air at zero distance from plate in Btu/hr ft²°F.

$\left. \frac{dT}{dx} \right|_{x=0}$: Temperature gradient of air at zero distance from plate in °F/ft.

Q : Quantity of heat conducted in Btu/hr.

A : Area of plate in ft².

Now this heat flux is transferred to the air below and we can write:

$$\frac{Q}{A} = - k_a \left. \frac{dT}{dx} \right|_{x=0} = h_c (T_s - T_\infty) = h_c \Delta T \quad (13)$$

where h_c : Heat transfer coefficient in Btu/hr ft²°F

T_s : Plate bottom surface temperature in °F

T_∞ : Ambient temperature in °F

Thus by obtaining $\left. \frac{dT}{dx} \right|_{x=0}$ from the graphs presented in Figures (13) to (18) , and by evaluating k_a from standard tables for the properties of air at the temperature of the test plate Q/A was determined. Using this heat flux value, the heat transfer coefficient h_c was computed by dividing Q/A by $(T_s - T_\infty)$. For values of T_s , the temperature gradient curves obtained from the temperature scans plotted in Figures (13) to (18), were extrapolated to obtain the ΔT at zero distance from the plate which yielded the temperature of the air at the test plate when the ambient temperature was added. It may be noted here that this temperature could also be obtained directly with the probe by touching the junction to the plate but this reading was observed to be about 1% lower than the one obtained by extrapolation. This temperature drop was thought to be due to a fin effect caused by the wires on touching the plate. The value obtained by extrapolation in the manner indicated above was compared with the average value of the plate temperature obtained from the eighteen embedded thermocouples. An average of this value and the value obtained by extrapolation was taken as the value of T_s , the plate surface temperature.

The ambient temperature T_∞ was measured by removing the probe from the test surface. This reading was periodically compared with the value of the ambient temperature read from a mercury-in-glass thermometer and was found to be within $\pm 1^\circ F$ of the ambient temperature.

The values of T_s and T_∞ determined as explained above enabled the temperature difference ($T_s - T_\infty$) to be evaluated for each particular value of heat flux, and enabled the corresponding heat transfer coefficient h_c to be determined by Equation (13)

The following equations were then used to evaluate the dimensionless parameters.

$$Nu = \frac{h_c \ell}{k} \quad (14)$$

$$Gr = \left(\frac{g \beta \rho^2}{\mu} \right) \times \Delta T \times \ell^3 \quad (15)$$

where

Nu: Nusselt number

Gr: Grashof number

ℓ : Characteristic length of the plate taken as the side length in ft.

k: Thermal conductivity of air in Btu/hr ft^{°F}

g: Gravitational constant taken as 32.16 ft/sec²

β : Coefficient of thermal expansion of air in 1/°F

ρ : Density of air in lbm/ft³

μ : Viscosity of air in lbm/ft sec.

All these air properties were evaluated at the film temperature $T_f = 1/2(T_s + T_\infty)$. The values of the Prandtl number Pr used to evaluate Grashof Prandtl number product were taken from standard air properties tables at the film temperature.

6. RESULTS

The results obtained by this experimental study are presented in this section.

The temperature profiles obtained from the temperature scans below the plate are shown in Figures (13) to (18) which are plots of temperature difference ΔT versus displacement x . These plots enabled the evaluation of $\left. \frac{dT}{dx} \right|_{x=0}$, the slope of the profiles at zero displacement as explained previously. For each set of experiments corresponding to 0", 1/2" and 1" wide edge strips respectively, two figures are given, one representing the temperature profile for the highest temperature difference and the other representing the remainder of the temperature profiles for the other temperature differences. This procedure had to be adopted since the scale which had to be used for highest temperature difference did not permit the other profiles to be presented as advantageously as possible.

Two sets of plots, Figures (19) and (20) are presented correlating heat flux Q/A with temperature difference ΔT . These figures differ only with respect to manner in which heat flux was computed. Figure (19) presents a plot in which the values of heat flux were computed on the assumption that the plate was transferring a uniform heat flux over the entire area corresponding to the magnitude computed at the geometric centre. In actual fact it was found that the heat flux was uniform over 75% of the area while the remaining

25% of the area near the edges transferred heat at a different rate. Figure (20) presents a plot in which a discrete heat flux assumption was considered in the calculations as explained below. Figure (21) shows that the temperature distribution in the air below the plate is similar in the centre, side and corner locations up to about 7" from the edges. This observation implies that the heat flux transferred within this area is uniform while the dashed curves in Figures (13) to (18) show that the temperature profiles at the sides and the corners at about 1-1/2" from the edges are different than the temperature profiles at the centre. However, at low temperature difference levels, namely about 5°F and 10°F, the temperature distributions at all the locations were found to be the same, within $\pm 1\%$ difference at any location. Therefore, for these cases, the dashed curves are not presented in Figures (13) to (18).

The observations above lead to the assumption that the area of the plate comprised of a 3" wide region around the edges, which transferred heat at the rate which was computed using the temperature profiles obtained at the corner or the side, while the rest of the area (which was 75% of the total area of the plate) transferred heat at the rate, which was computed using the temperature profile obtained at the centre of the plate. This discrete heat flux assumption was used in the calculations for the plot of Figure (20). With such a consideration, the maximum increase in the overall heat flux was approximately 12% for the no fin configuration and approximately 4% for the case of the 1/2"

fin configuration while the maximum decrease for the case of the 1" fin configuration was found to be approximately 8%. The maximum changes were found to occur at the highest temperature difference level.

An energy balance was also performed for the system considering the heat input to the system as measured in terms of electric power supplied to heaters, the heat flux transferred downwards by the plate and all other losses. This analysis is presented in Appendix B for two tests corresponding to the no fin configuration. The discrepancy is only about 8 % of the electrical power which could easily be accounted for by the heat losses through the supports, and approximations and assumptions used in the calculation procedures for various losses.

Furthermore, to verify the existence of the thermal boundary layer below the plate and to obtain a qualitative measurement of its thickness, Schlieren photographs were taken as presented in Figures (22) and (23). Figure (22) presents a photograph taken with the Schlieren apparatus aligned with the centre portion of the plate. As indicated on the photograph, the thickness of the boundary layer is of the order of seven tenths of an inch which confirms the values obtained by probe measurements.

Figure (23) presents the photograph taken with the Schlieren apparatus aligned with the edge of the test plate which appears about one quarter of the way across the photograph. This photograph distinctly indicates the thinning of the boundary layer near the edge, again confirming the probe measurements.

7. DISCUSSION

7.1 Accuracy Of Results:

This section concerns the analysis of the uncertainties in the experimental study and their bearing on the final results. Maximum possible error was computed in the analysis in each case which gave a high percentage of uncertainty. Maximum possible error results as a consequence of the improbable combination of the maximum values of the individual uncertainties in the various measurements.

The fluid property values used in calculating the dimensionless parameters were assumed to be those of dry air though humidity might have run as high as 80% during the experimentation. This undoubtedly would have introduced some error in the results but has not been considered in this analysis. The error involved in determining a particular property value at a certain temperature (interpolating between published values) was minimized by fitting a ten degree polynomial between eleven known property values published in the range between 0°F to 400°F at 40°F intervals given in Reference (11). The interpolation error has been considered in the analysis as well.

The uncertainty analysis is presented below.

<u>Description of Uncertainty</u>	Maximum % Uncertainty ($\Delta T = 5^\circ F$)	Maximum % Uncertainty ($\Delta T = 25^\circ F$)
(A) <u>Value of Temperature Difference</u>		
$\Delta T = (T_s - T_\infty)$		
Plate Surface Temperature		
(i) Thermoelectric Error	± 0.2	± 0.2
(ii) Potentiometer Inaccuracy	± 0.1	± 0.2
(iii) Reading Error	$\pm 0.2^*$	$\pm 0.5^\dagger$
Ambient Temperature		
(i) Thermoelectric Error	± 0.2	± 0.2
(ii) Potentiometer Inaccuracy	± 0.1	± 0.2
(iii) Reading Error	± 0.2	± 0.2
Total Error in Temperature		
Difference#	± 16.0	± 1.4
(B) <u>Value of Heat Flux</u>		
$\frac{Q}{A} = -k_a \left. \frac{dT}{dx} \right _{x=0}$		
Thermal Conductivity		
(i) Film Temperature Uncertainty	± 1.0	± 1.7
(ii) Interpolation Error	± 0.1	± 0.1

* Low temperature readings were made with potentiometer

† High temperature readings were taken from recorder paper

Total Error % = $(\text{Absolute error in } T_s + \text{Absolute error in } T_\infty) \times (100) / \text{Temperature Difference}$

Temperature Gradient	Maximum % Uncertainty ($\Delta T = 5^\circ\text{F}$)	Maximum % Uncertainty ($\Delta T = 250^\circ\text{F}$)
(i) Probe Reading		
Thermoelectric Error	± 0.2	± 0.2
Conduction and Radiation Losses	± 0.1	± 0.2
Potentiometer Accuracy	± 0.1	± 0.2
Reading Error	± 0.2	± 0.5
(ii) Estimation of Gradient from Plot	± 8.0	± 5.0
Total Error in Heat Flux	± 9.7	± 7.9

(C) Nusselt Number

$$\text{Nu} = \frac{h_c \ell}{k} = \frac{Q/A}{\Delta T} \cdot \frac{\ell}{k}$$

Heat Flux

Error ± 9.7 ± 7.9

Temperature Difference

Error ± 16.0 ± 1.4

Thermal Conductivity

Error ± 1.1 ± 1.8

Total Error

 ± 26.8 ± 11.1 (D) Grashof And Prandtl Number

$$\text{Gr} = \left(\frac{\alpha \beta \rho^2}{\mu} \right) (\Delta T) \ell^3$$

$$\text{Pr} = \frac{\mu C_p}{k}$$

	Maximum % Uncertainty ($\Delta T = 5^\circ F$)	Maximum % Uncertainty ($\Delta T = 250^\circ F$)
Physical Properties		
Interpolation Error	± 0.6	± 0.5
Temperature Difference		
Error	± 16.0	± 1.4
Characteristic Length		
Measurement Error	± 0.6	± 0.6
Total Error	± 17.2	± 2.5

7.2 Heat Flux Correlation:

The heat flux plots in Figure (19) and (20) indicate the following type of correlation between heat flux and temperature difference

$$Q/A = c(\Delta T)^d \quad (16)$$

The values of the coefficient and the exponent obtained for various cases are listed in the figures mentioned and are tabulated below.

TABLE I
Tabulation Of Empirical Constants

	Description Of Edge Restraints	Uniform Heat Flux Assumption		Discrete Heat Flux Assumption	
		c	d	c	d
1	No Edge Strip	.105	1.25	.102	1.27
2	1/2" Edge Strip	.106	1.23	.104	1.25
3	1" Edge Strip	.107	1.20	.116	1.16

Using Fishenden and Saunders (8) relationship as modified by McAdams, the correlation below can be written

$$Nu = 0.27 (Gr Pr)^{1/4} \quad (17)$$

$$\frac{h_c \ell}{k} = 0.27 \left[\frac{g \beta \rho^2}{\mu} \Delta T \ell^3 Pr \right]^{1/4} \quad (18)$$

Since $Q/A = -k_a \left. \frac{dT}{dx} \right|_{x=0} = h_c \Delta T$ (19)

$$\frac{Q/A}{\Delta T} \frac{\ell}{k} = 0.27 \left[\frac{g \beta \rho^2}{\mu} Pr \right]^{1/4} [\Delta T]^{1/4} [\ell]^{3/4} \quad (20)$$

$$Q/A = \frac{0.27 \left[\frac{g \beta \rho^2}{\mu} Pr \right]^{1/4} k}{\ell^{1/4}} (\Delta T)^{1.25} \quad (21)$$

Using the relationship expressed in Equation (21) by substituting the values of temperature difference for the present experimental study, a plot was drawn which is shown in Figure (24) and gave values of c and d as 1.05 and 1.23 respectively. The value 1.23 is lower than 1.25 showing that the fluid properties do affect the exponent. The experimental values in general are in good agreement with Fishenden and Saunders correlation with maximum 6.6% and 16.8% deviation corresponding to uniform heat flux assumption and discrete heat flux assumption for the case of plate with no edge restraints.

7.3 Effect Of Edge Restraints:

As observed from Figure (19) and (20), the edge strips tend to decrease the overall heat flux. However, the experimental evidence

supporting the functional relationship is insufficient to justify another correlation for plates with edge restraints. At the same time, it can be recommended safely that the overall heat transfer does tend to decrease with edge restraints.

Considering the effect of edge restraints, intuitively it would appear quite reasonable that edge restraints would reduce heat flux since the edge restraints tend to stop the flow of air from edges thus increasing the thickness of boundary layer and decreasing temperature gradient at the surface.

Fishenden and Saunders (8) indicated that for the case of a horizontal plate facing downwards, were it not for edge effects and slight irregularities of temperature over the plate surface, there would be no convection currents, since the layer of warm air near the plate would be in equilibrium in a draught free room, although heat would, of course, still be lost from the plate by conduction. It may be realized that if the gross movement of air is prevented or the hot air is prohibited from escaping from the sides of the plate, the heat transfer from the plate will be by conduction. The heat transfer coefficient in such a case will be much lower than that for convection. Hence the trend for heat transfer coefficient to decrease with edge restraints is reasonable.

7.4 Nusselt Number Correlation:

As already mentioned in the literature survey, Fishenden and Saunders (8) gave a correlation for Nusselt number which

depended on the Grashof Prandtl number product raised to the power 0.25 multiplied by a coefficient of 0.25 for the horizontal plate facing downwards. Figures (25) and (26) present Fishenden and Saunders correlation as a solid line and show the scatter of the data points obtained from the present study. For the plate without edge restraints, the maximum deviations are $\pm 7\%$ and $\pm 20\%$ for the case of the uniform heat flux assumption and the discrete heat flux assumption respectively.

7.5 Air Temperature Fluctuations:

It has already been mentioned that fluctuations were detected by the thermocouple probe measuring the temperature of the air below the test plate. Samples of recorder paper were also presented in Figures (10), (11) & (12). Figure (27) further shows the envelope around the mean value curve drawn through the maximum and minimum values observed. The general pattern of the fluctuations remained the same for all tests but the relative magnitudes were less for lower temperature difference levels as indicated in Figures (10), (11) & (12). The following reasons could account for the above mentioned fluctuations.

- (i) The movement of the thermocouple junction by the flow of hot air. Thermocouple junction moved as much as $\pm .002$ " from its position of rest. This movement was observed by an optical instrument.
- (ii) The disturbances in the flow pattern itself induced by casual movements in the room. Due to the existence of

a temperature gradient below the plate , Such a disturbance would cause mixing of air of different temperatures, resulting in a variation of temperature at the thermocouple junction.

It can also be noticed that the fluctuations are minimal up to about .02" from the plate because of the air movement being damped by the presence of the stationary plate. Then further from the plate, the fluctuations gradually start increasing, attaining a maximum value in the region where $\frac{d^2T}{dx^2}$ in the air is maximum and then again start decreasing, finally reducing to zero as the probe approaches ambient temperature. The fact that the fluctuations are maximum at the point where $\frac{d^2T}{dx^2}$ is maximum can be observed in Figure (27).

8. CONCLUSIONS

The experimental study of the free convection heat transfer from a heated horizontal plate facing downwards resulted in a correlation which in general agreed with the correlation given by Fishenden and Saunders as modified by McAdams.

$$Nu = 0.27 (GrPr)^{1/4}$$

The experimental study was further extended to study the effect of edge restraints on heat transfer and this study indicated that the heat transfer coefficient tended to decrease with the increasing height of edge restraints. However, no correlations were given because of insufficient experimental evidence.

9. REFERENCES

1. Brown, I. A. and S. M. Marco, "Introduction To Heat Transfer", McGraw-Hill Book Company, Inc.; 1958.
2. King, W. J., Mech. Eng., 54, 550 (May, 1932).
3. Jakob, M. and W. Linke, Forschung a.d. Geb. d. Ingenieurwes. 4, 75; 1933.
4. Jakob, M., "Heat Transfer", Vol. I, John Wiley & Sons, Inc. New, York, 1958.
5. Griffiths, E. and A. H. Davis, Department of Scientific and Industrial Research Food Investigation Board, special Rep. No. 9, His Majesty's Stationary Office, London, 1922.
6. Weise, R., Forschung a.d. Geb. d. Ingenieurwes. 6, 281; 1935.
7. Schmidt, E., Forschung a.d. Geb. d. Ingenieurwes. 6, 281; 1932.
8. Fishenden, M. and O. A. Saunders, "An Introduction To Heat Transfer", Oxford, 1950.
9. McAdams, W. H., "Heat Transfer", McGraw-Hill Book Company, Inc., New York, 1954.
10. Kutateladze, S. S. and V. M. Borishanskii, "A Concise Encyclopedia of Heat Transfer", Pergamon Press, 1966.
11. Grober, H. and S. Erk, "Fundamentals of Heat Transfer", McGraw-Hill Book, Company, Inc., 1961.
12. Kreith, Frank, "Principles of Heat Transfer", International Text Book Co., 1962.

10. ILLUSTRATIONS

TEST FACILITY FRONT VIEW

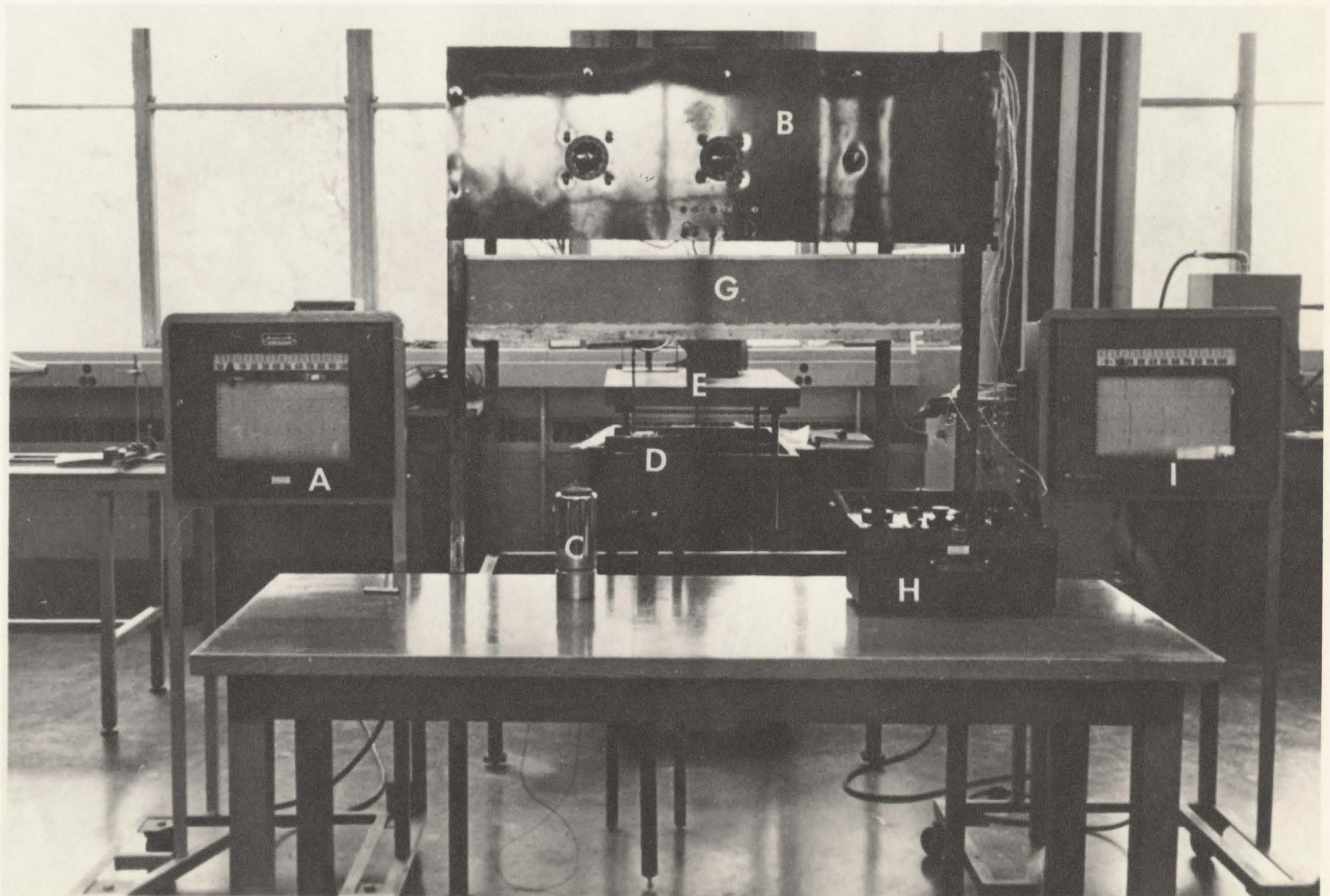


Figure #1

FIGURE #1

Test Facility Front View

Apparatus Description

- A - Single Point Recorder
- B - Front Panel Board With Variacs And Wattmeter Terminals
- C - Ice Bath
- D - Thermocouple Probe With Stand
- E - Schlieren Apparatus
- F - Test Plate
- G - Insulation Cover
- H - Potentiometer
- I - Twelve Point Recorder

TEST FACILITY SIDE VIEW

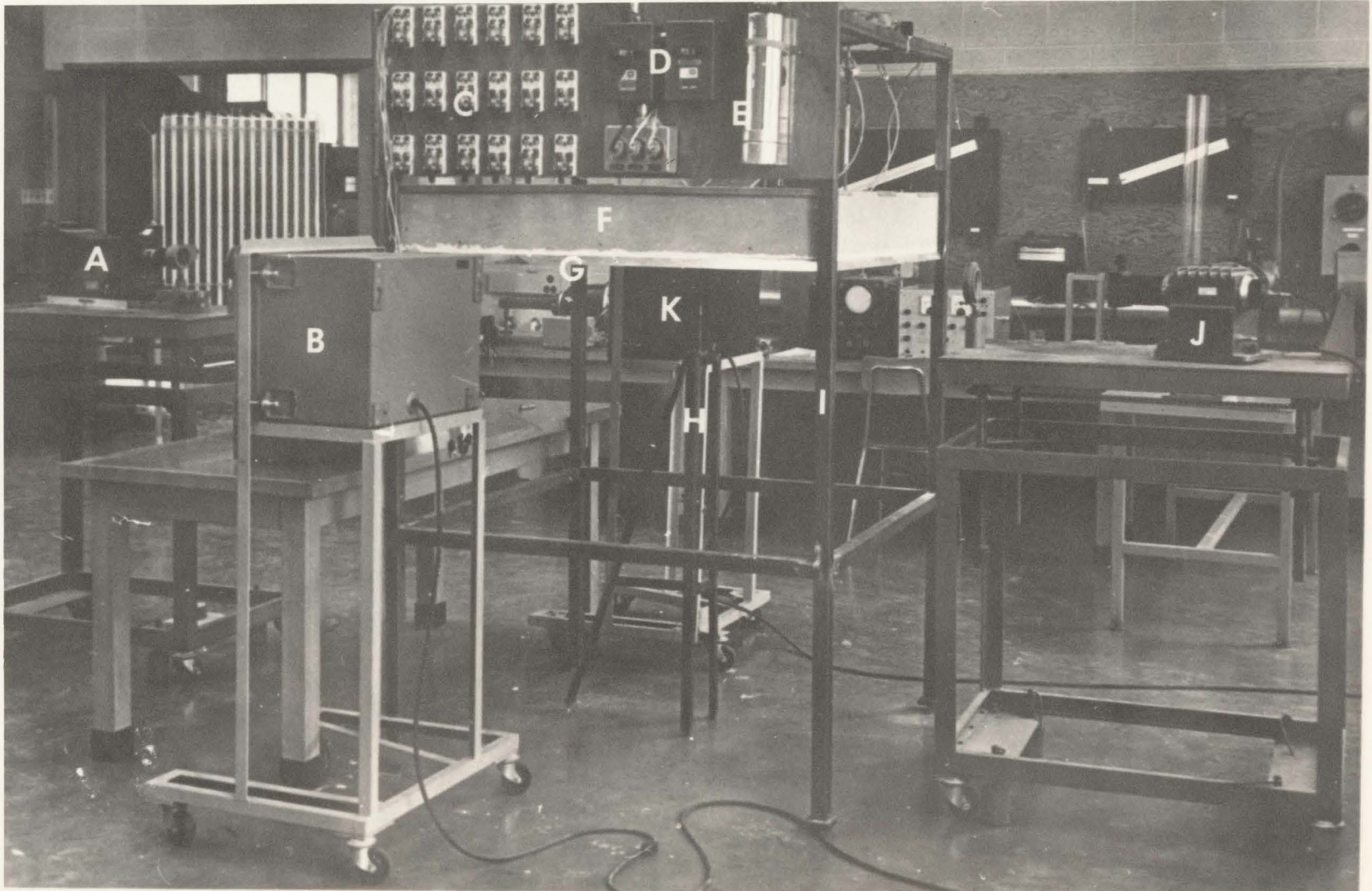
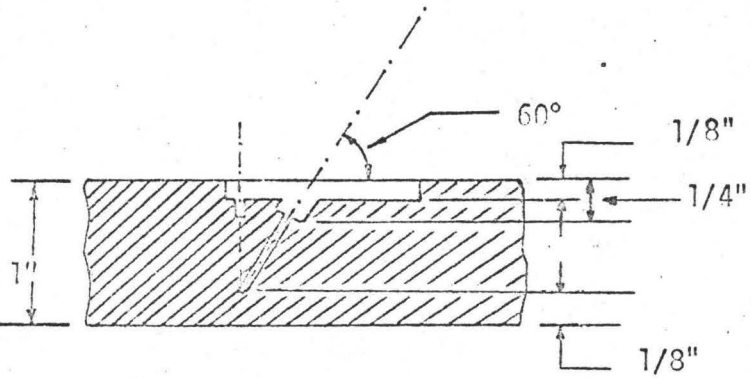


Figure #2

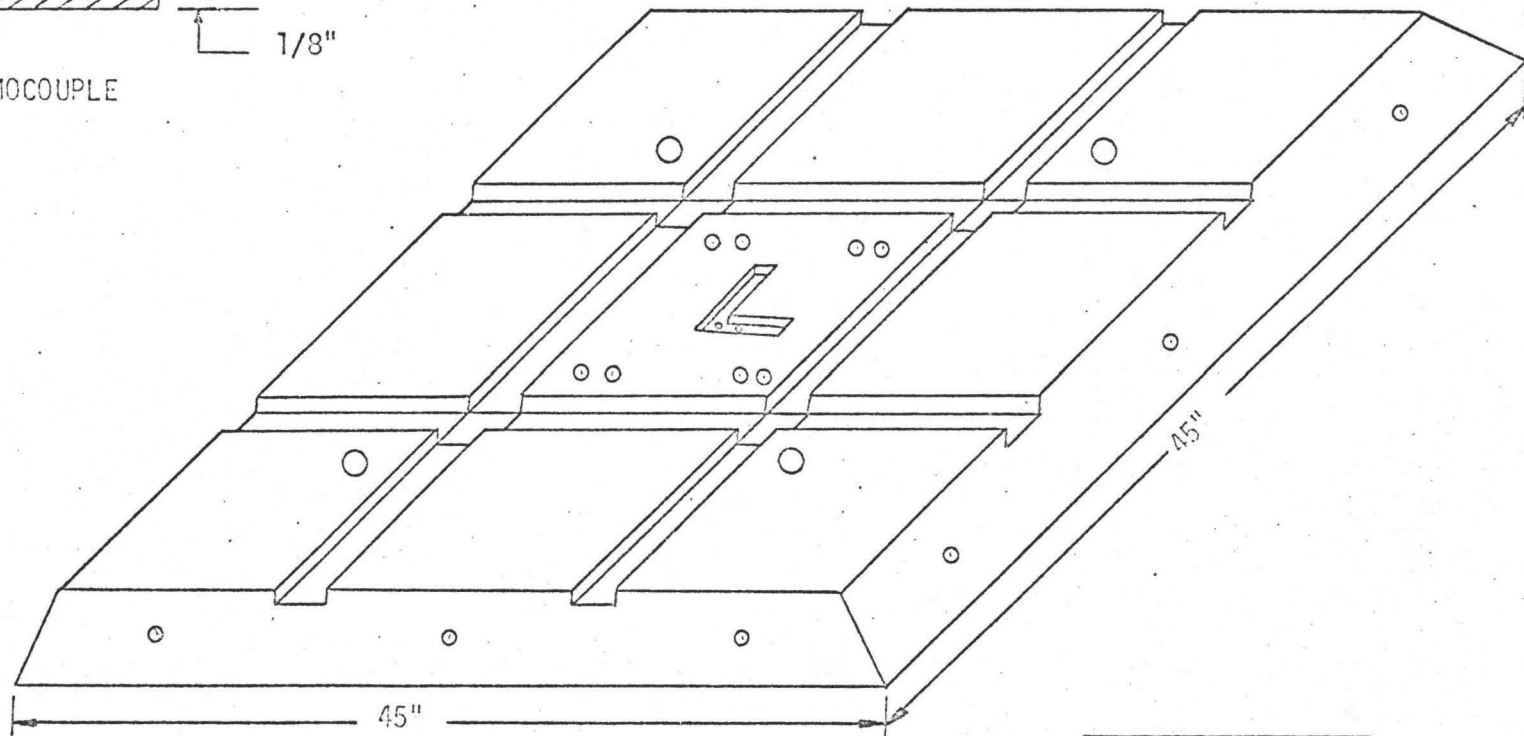
FIGURE #2
Test Facility Side View
Apparatus Description

- A - Schlieren Apparatus, Camera
- B - Twelve Point Recorder
- C - Knife Switches
- D - Fuses
- E - Ice Bath
- F - Insulation Cover
- G - Test Plate
- H - Thermocouple Probe With Stand
- I - Test Plate Stand
- J - Schlieren Apparatus, Light Source
- K - Single Point Recorder



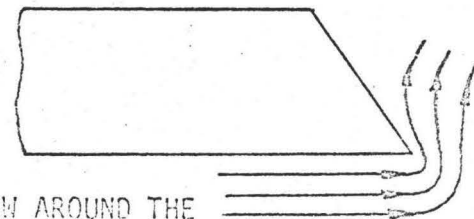
DETAILS FOR THERMOCOUPLE
HOLES

FIGURE #3(b)



TEST PLATE

Figure #3(a)



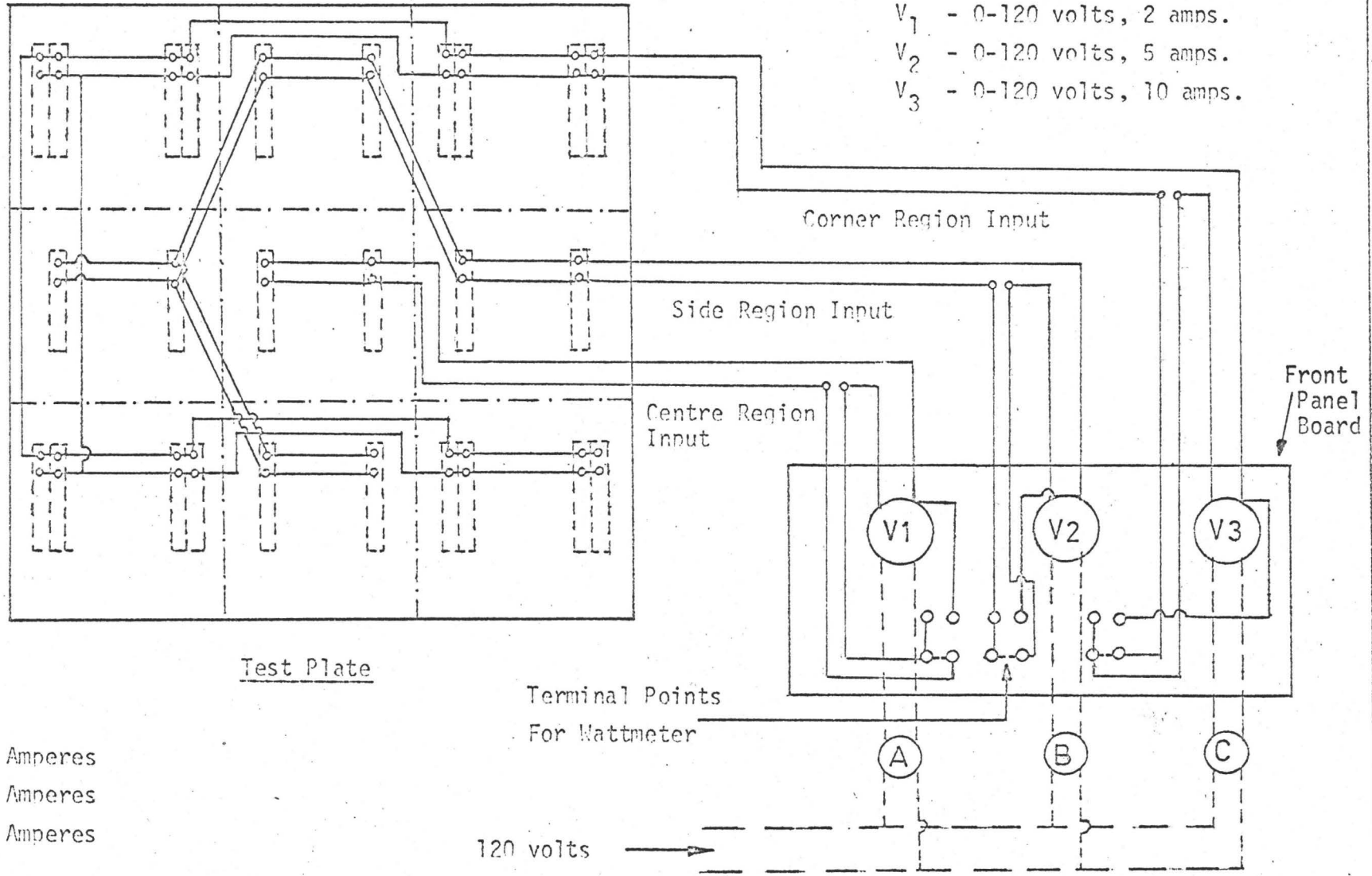
AIR FLOW AROUND THE
CORNER

FIGURE #3(c)

HEATER WIRING DIAGRAM

Power Variacs

- V₁ - 0-120 volts, 2 amps.
- V₂ - 0-120 volts, 5 amps.
- V₃ - 0-120 volts, 10 amps.



Fuses

- A 2 Amperes
- B 5 Amperes
- C 10 Amperes

Terminal Points
For Wattmeter

120 volts

FIGURE #4

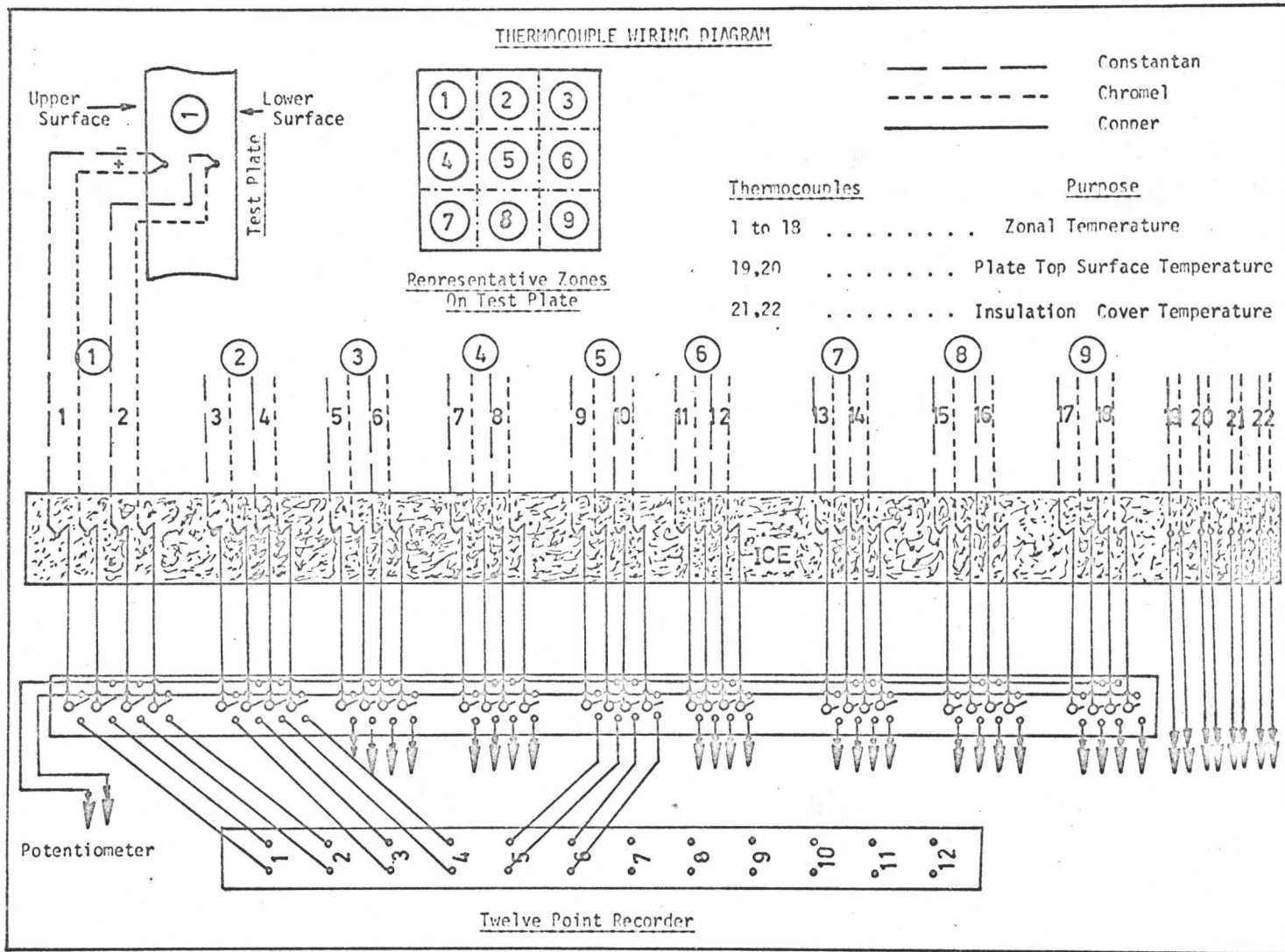


FIGURE # 5

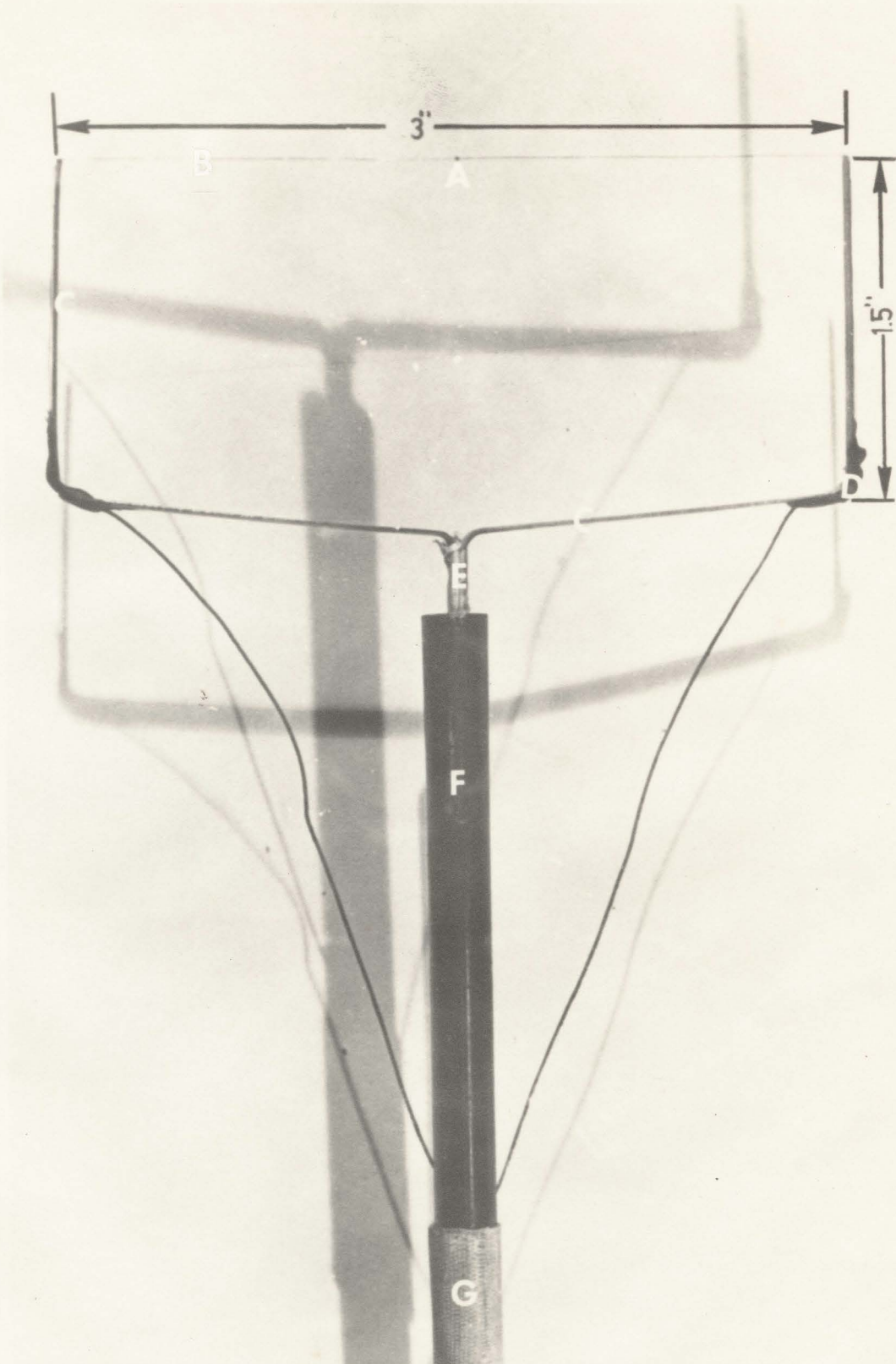


Figure #6

FIGURE #6

Thermocouple Probe

Apparatus Description

- A - Thermocouple Junction
- B - 40 Gauge Chromel Alumel Thermocouple Wire
- C - Probe Supports
- D - Instant Epoxy Holding Wire To Supports
- E - Teflon Insulation Tape To Insulate Supports From Each Other
- F - Rod
- G - Silicon Tape To Hold Wire To Rod

THERMOCOUPLE PROBE WITH STAND AND ACCESSORIES



Figure #7

FIGURE #7

Thermocouple Probe With Stand And Accessories

Apparatus Description

- A - Thermocouple Probe
- B - Traversing Attachment
- C - Stand
- D - Traversing Attachment Base

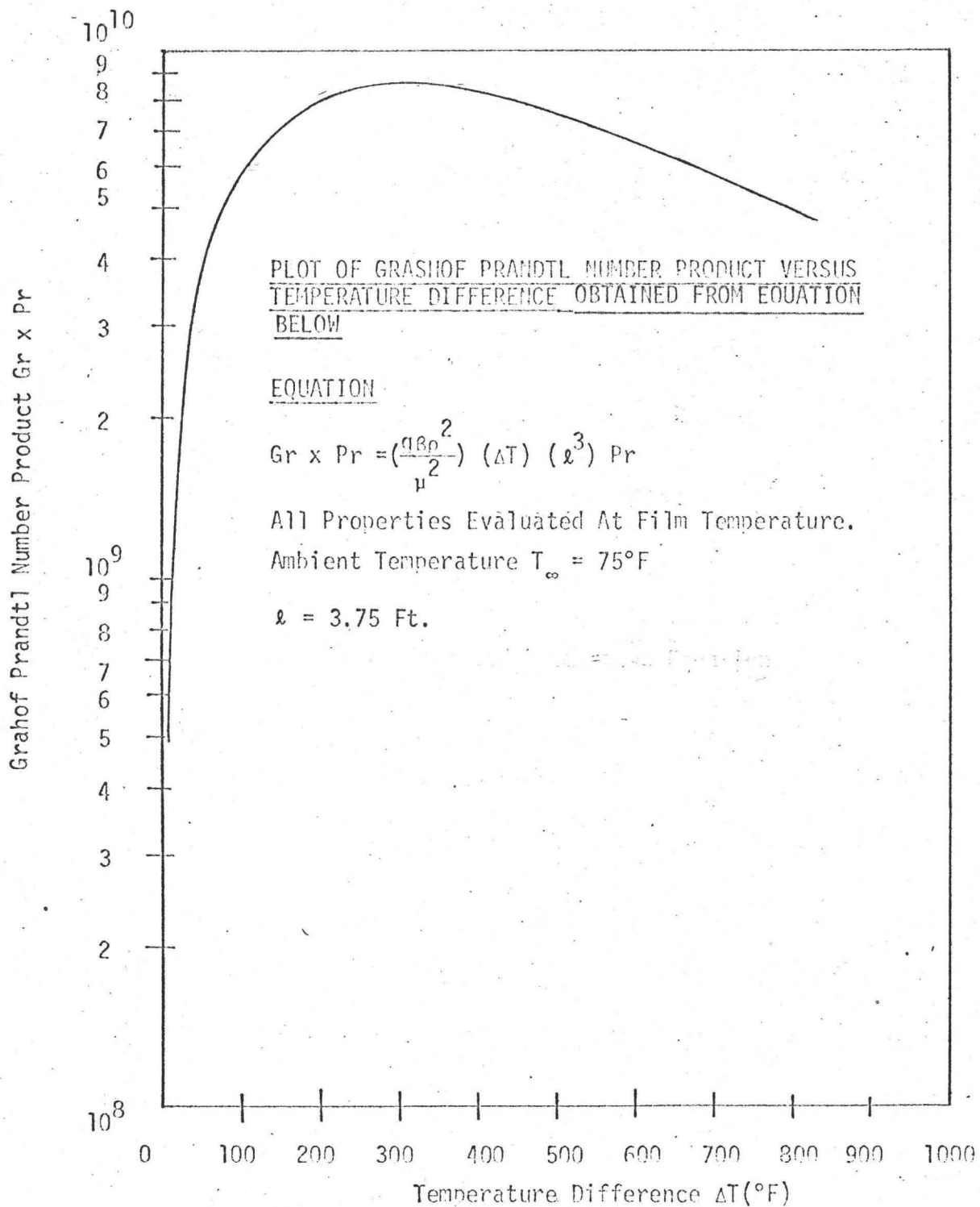
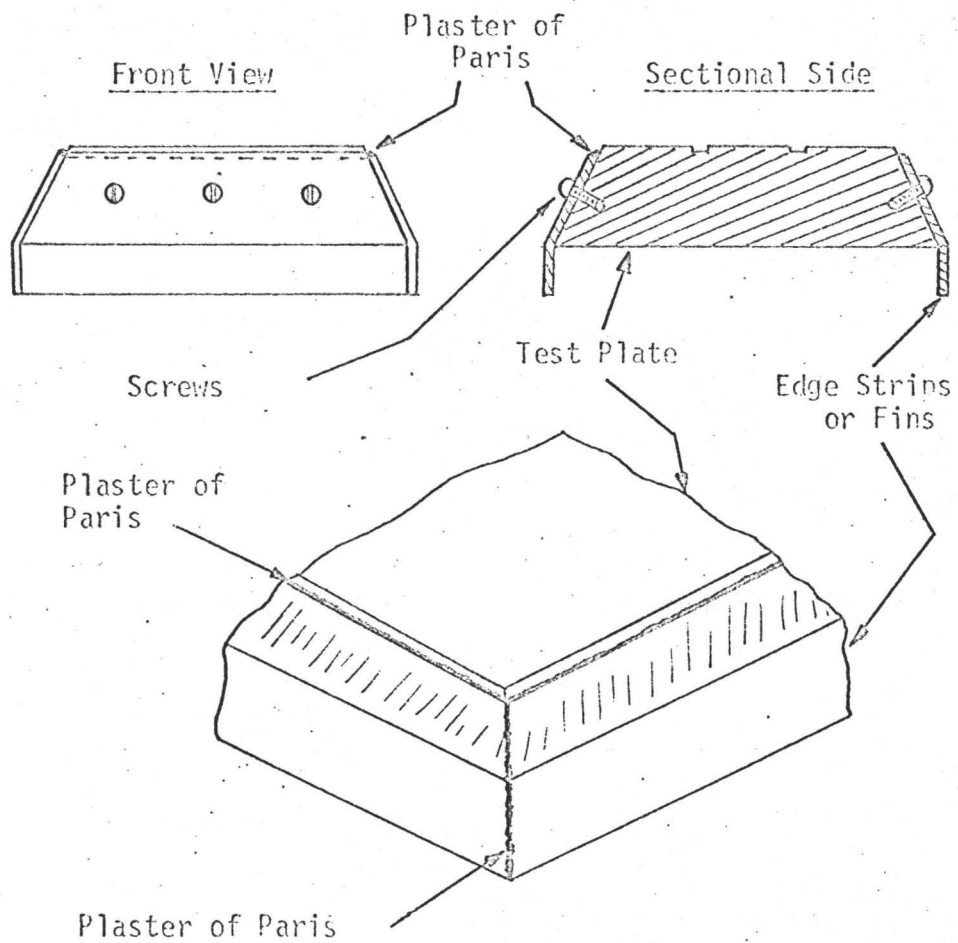


Figure 8

REPRESENTATIVE SKETCH OF FIN ARRANGEMENT

NOT TO SCALE

FIGURE # 9

TEMPERATURE RECORDING SAMPLES

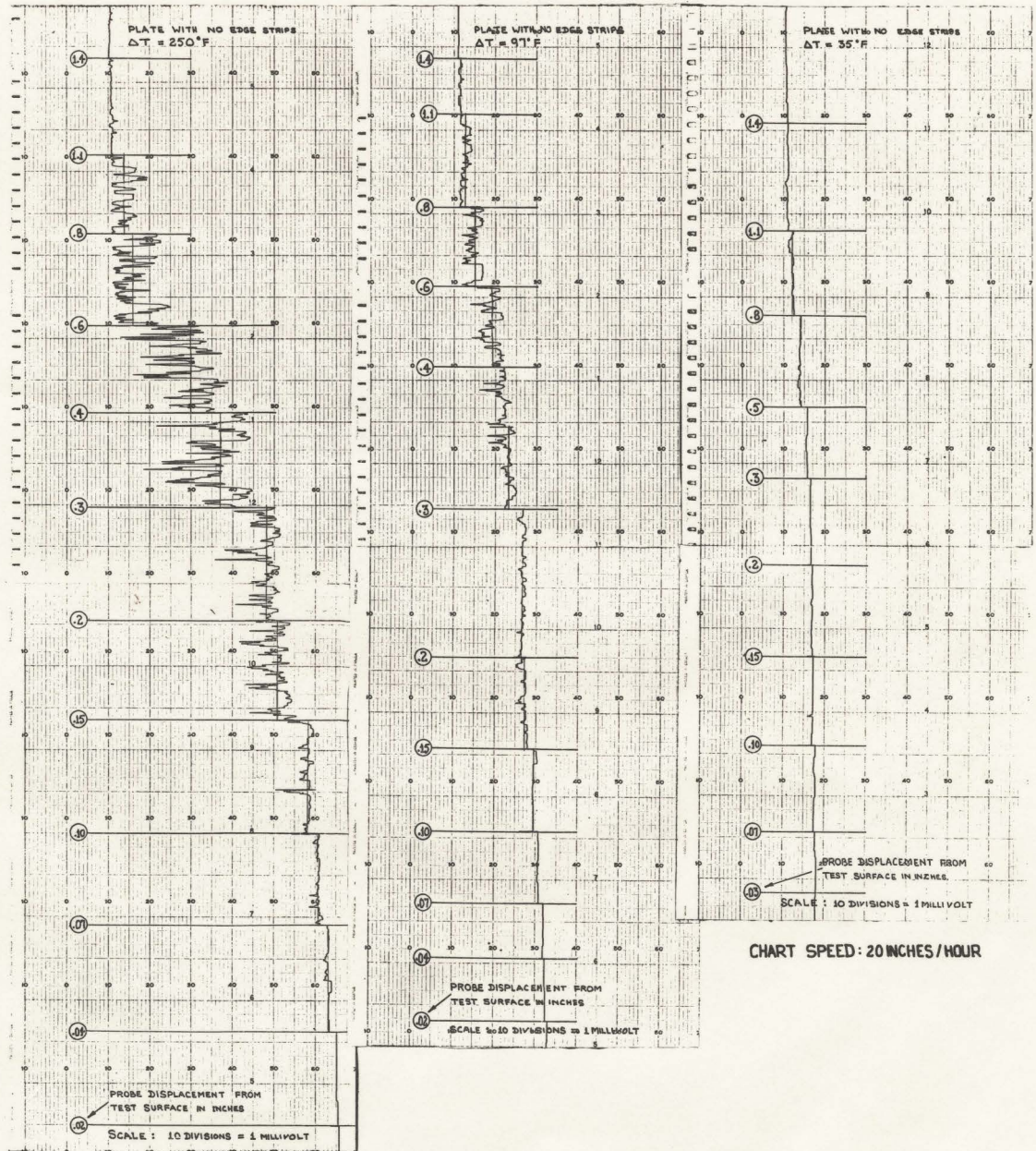


Figure #10

TEMPERATURE RECORDING SAMPLES

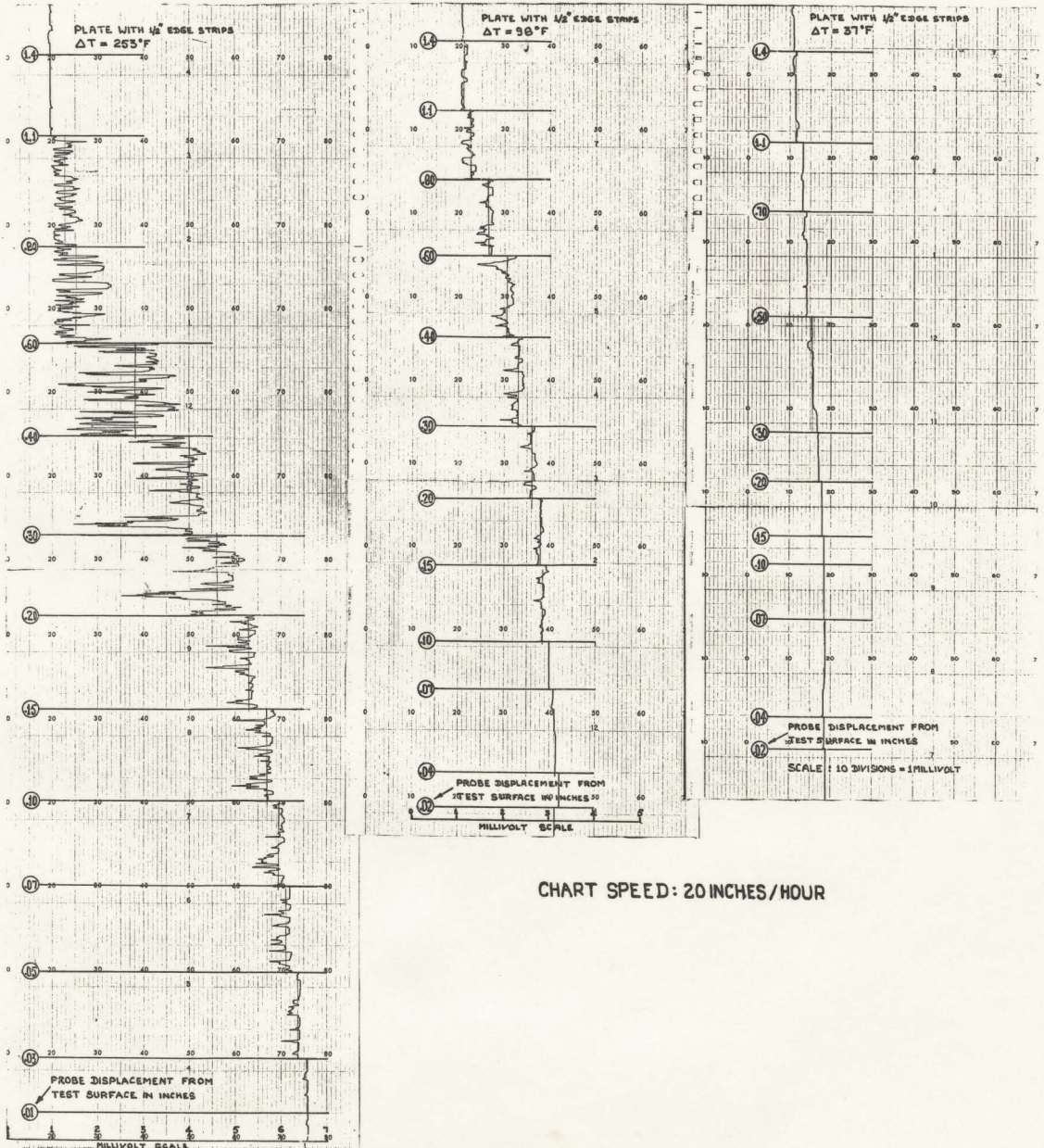


CHART SPEED: 20 INCHES/HOUR

Figure #11

TEMPERATURE RECORDING SAMPLES

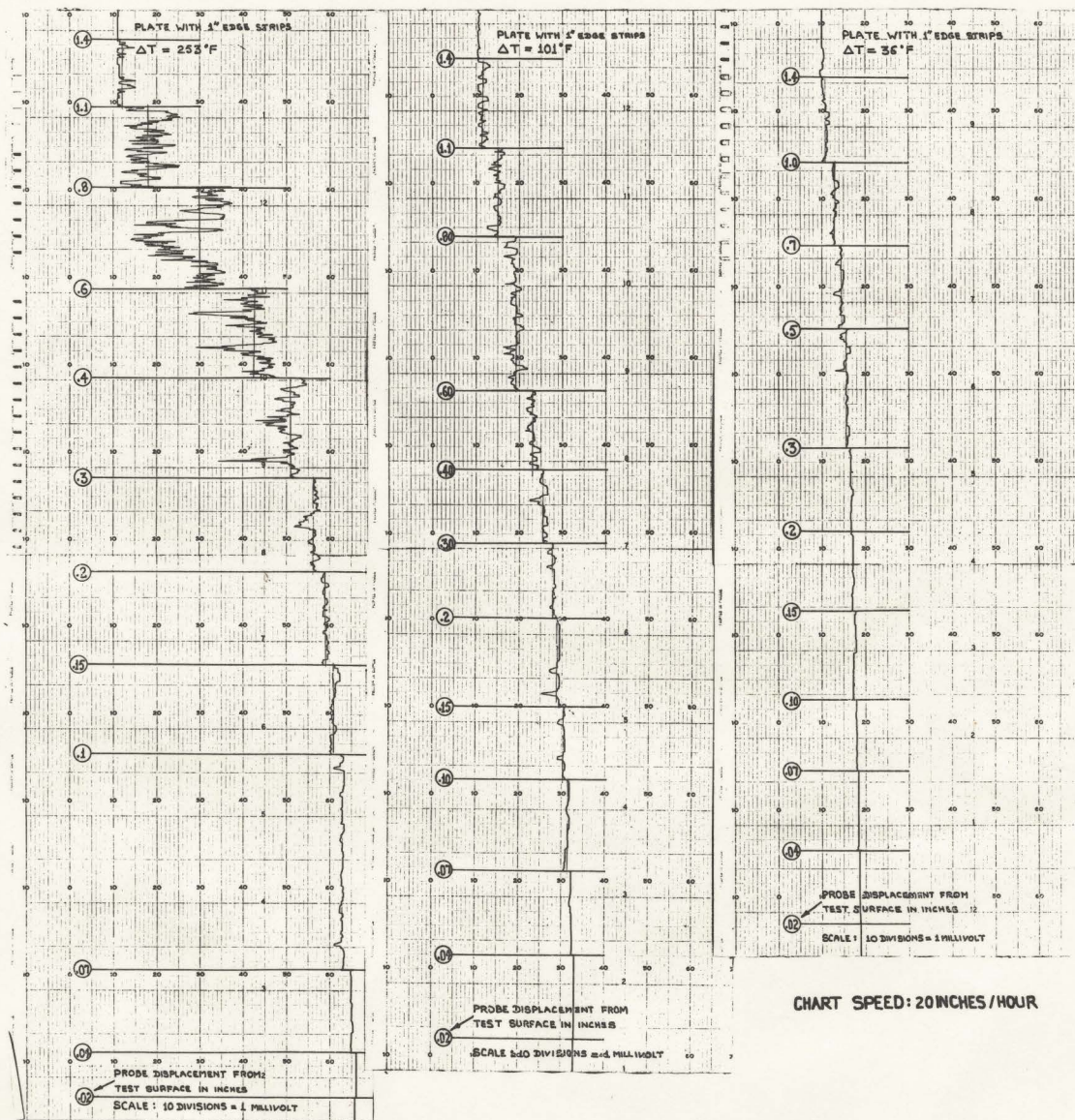


Figure #12

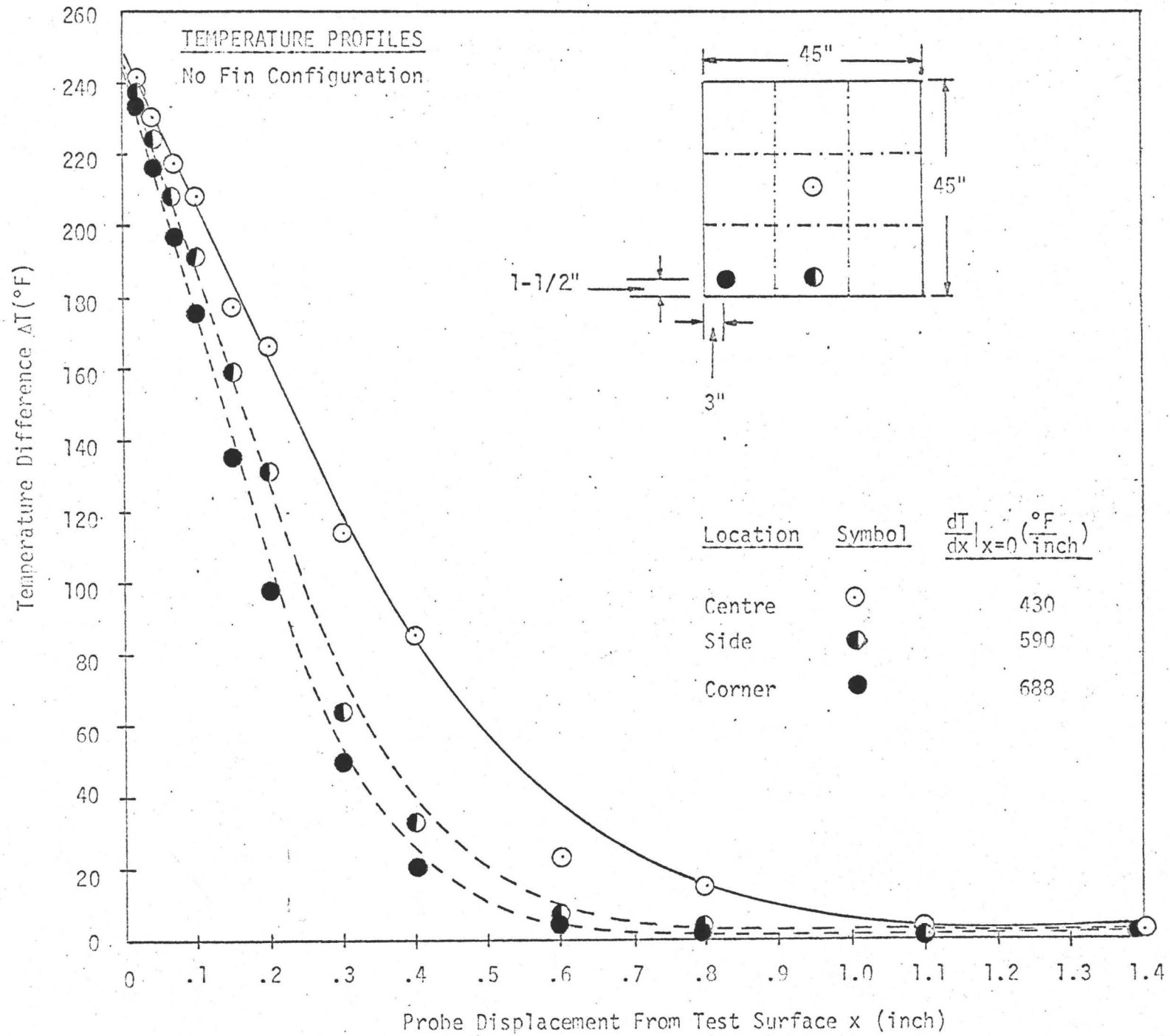


Figure 13

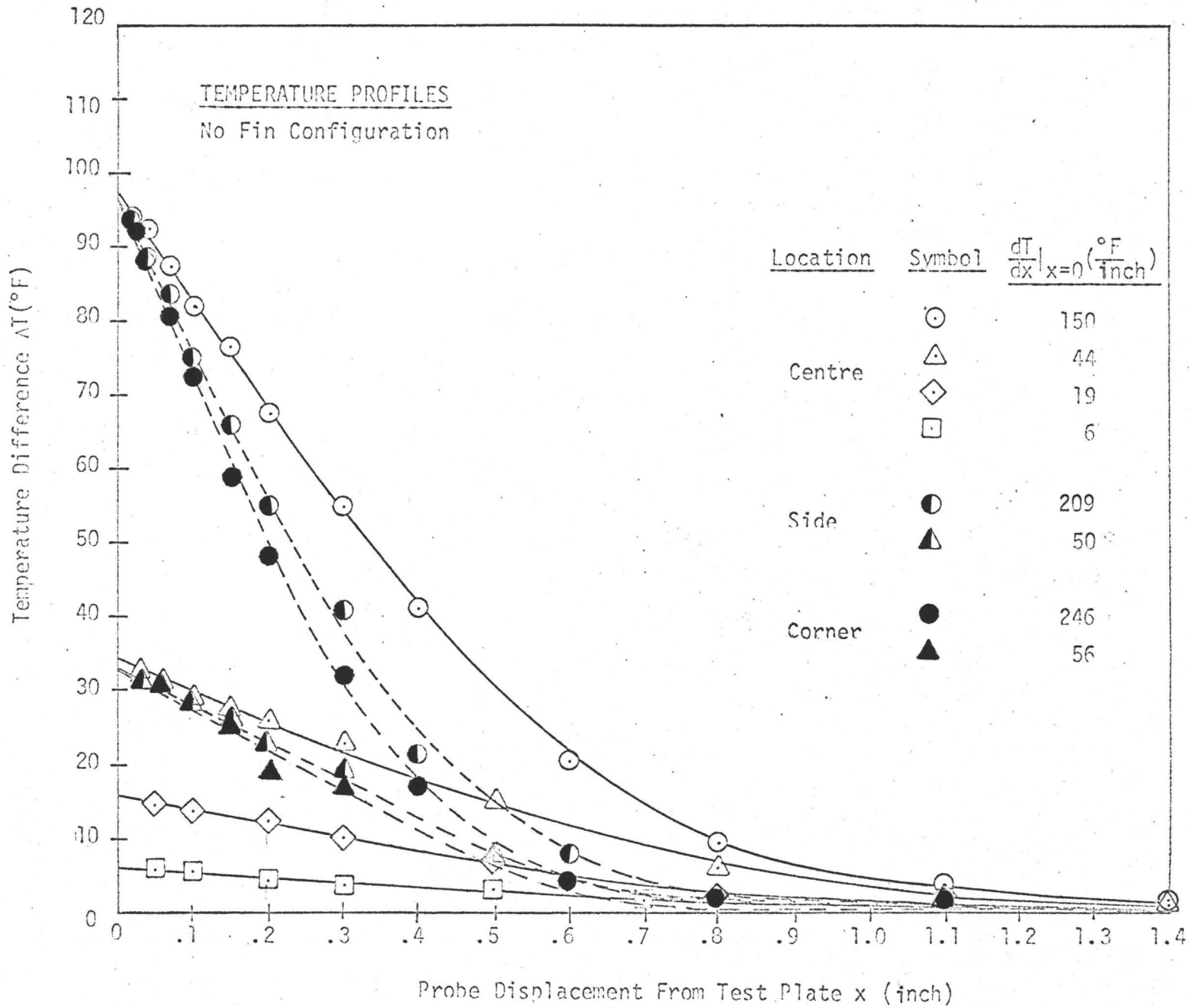


Figure 14

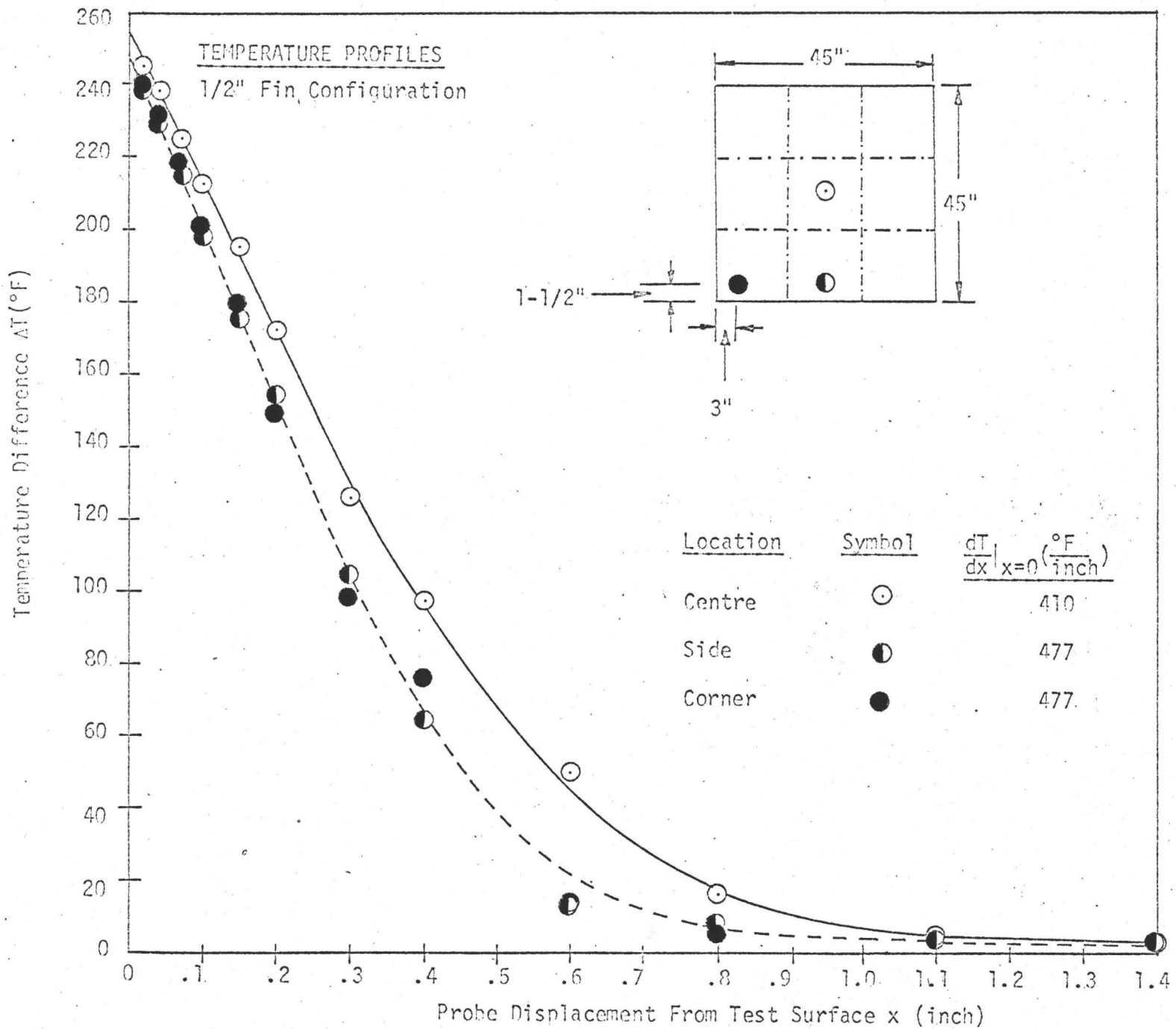


Figure 15

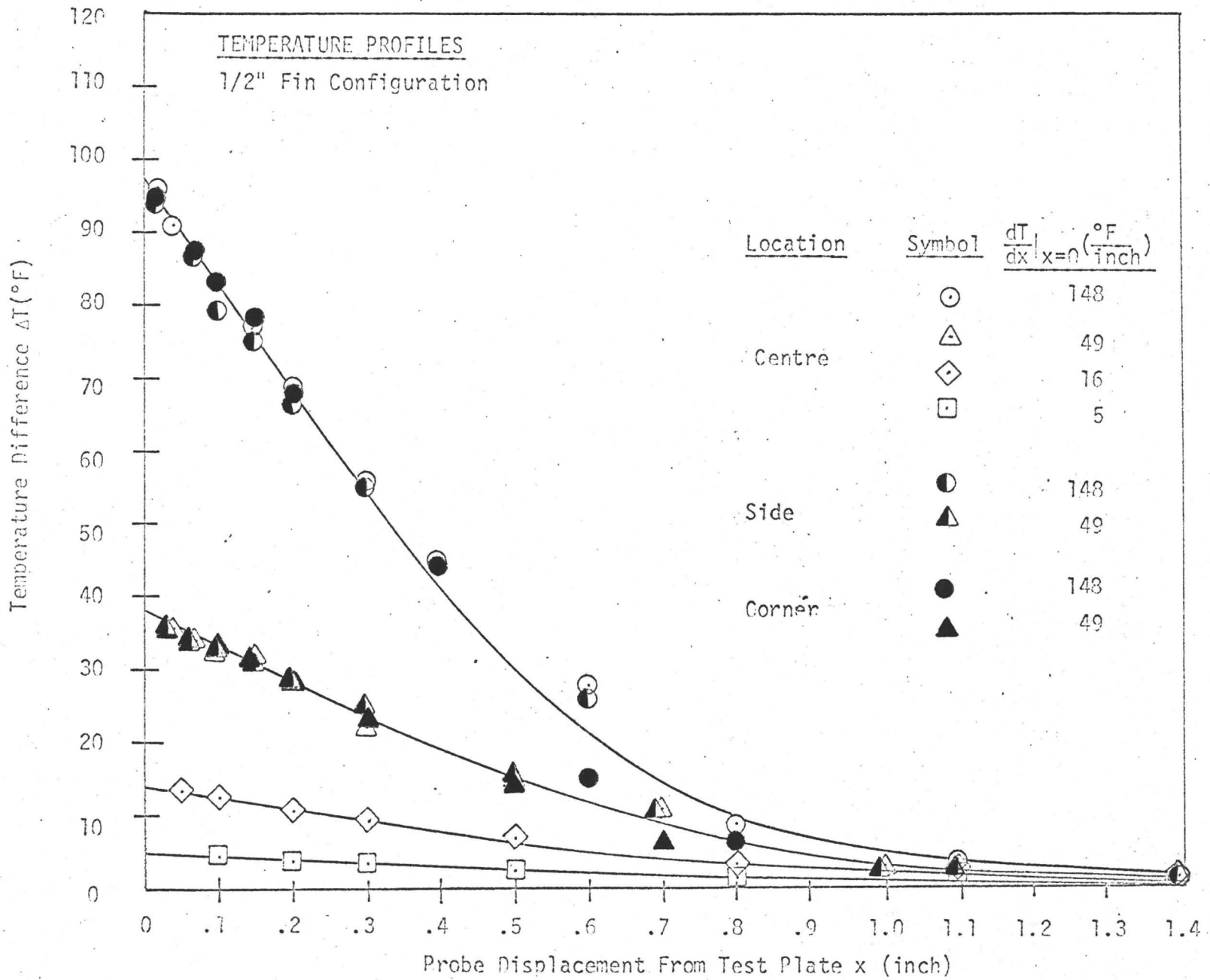


Figure 16

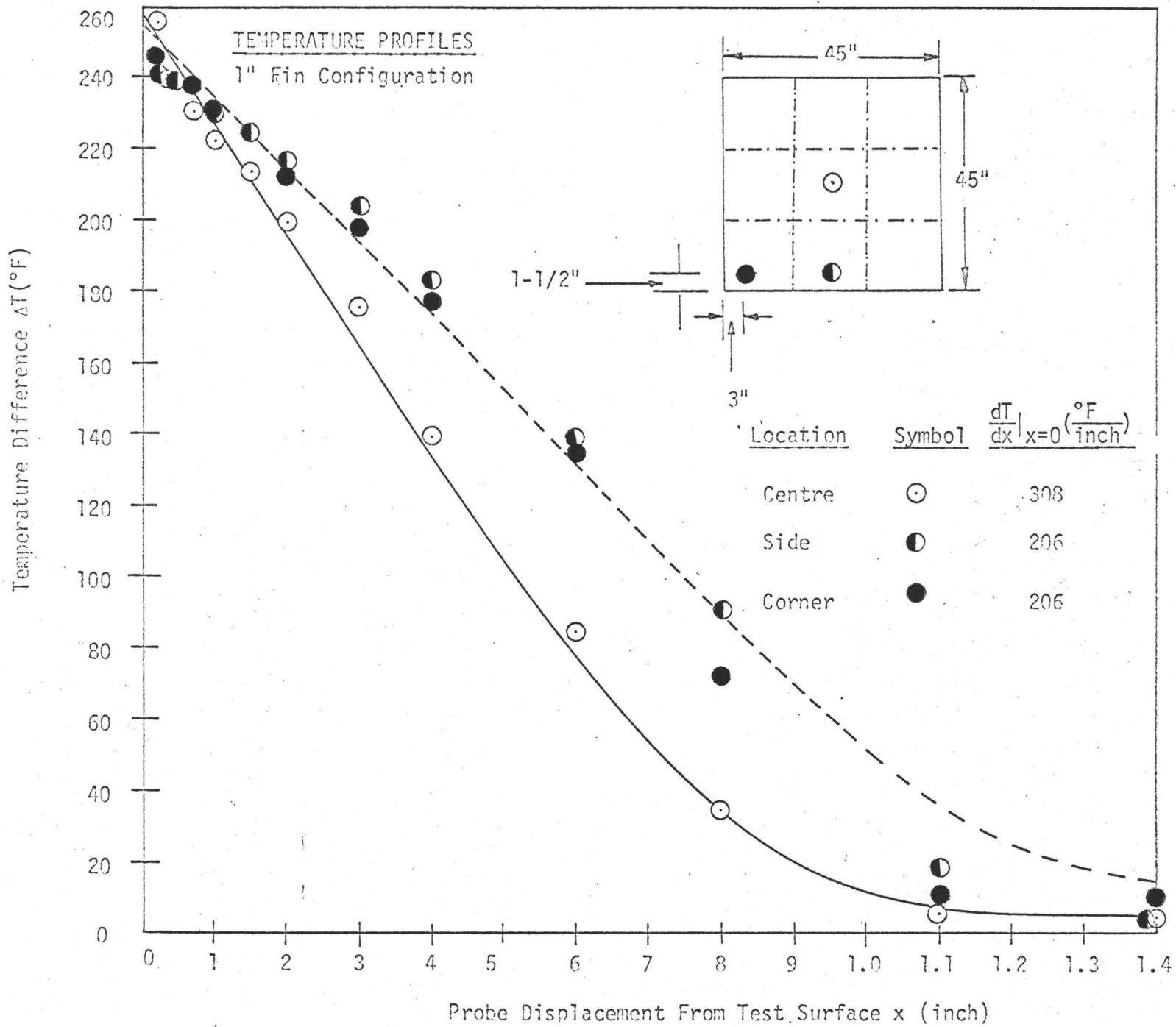


Figure 17

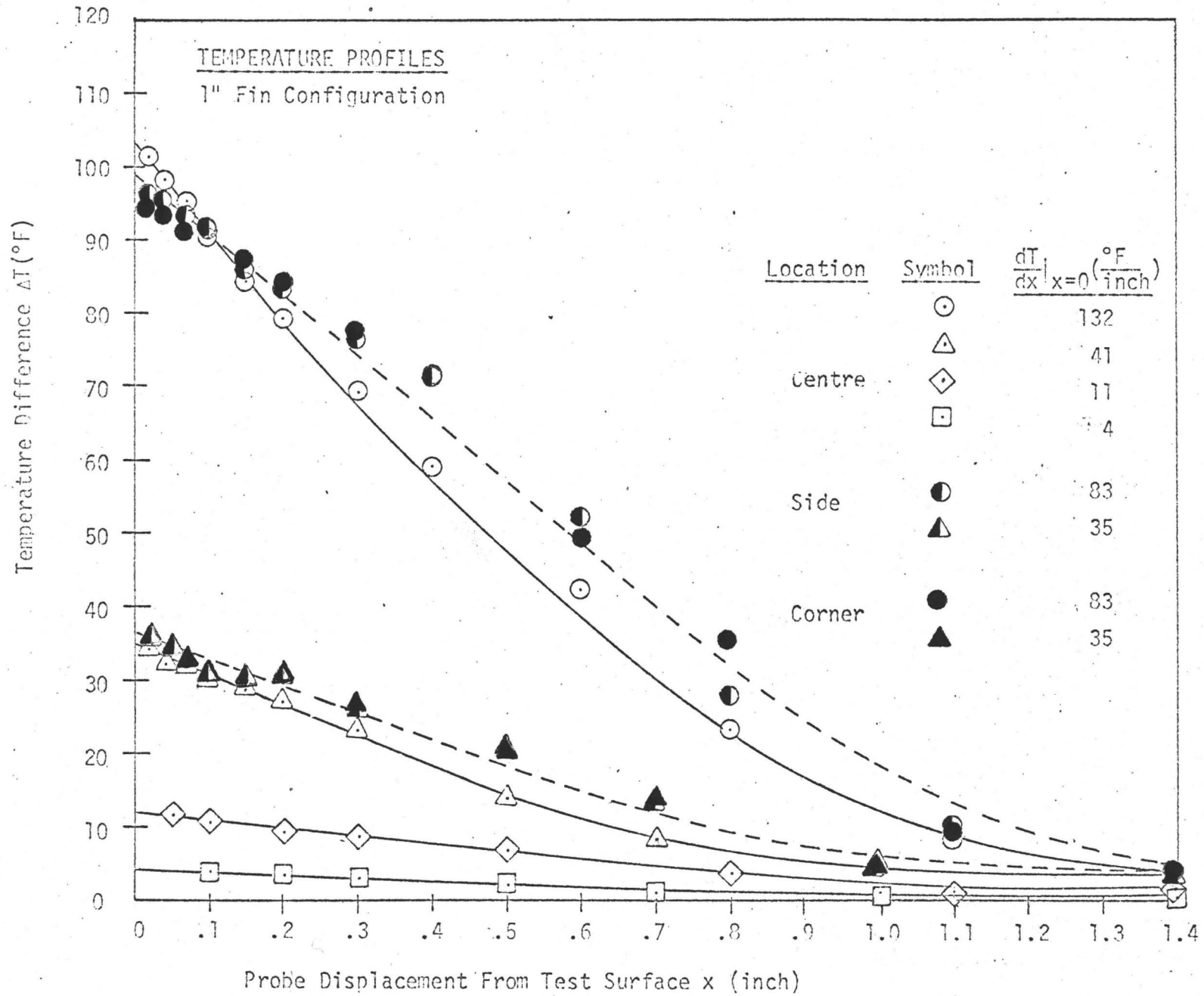


Figure 18

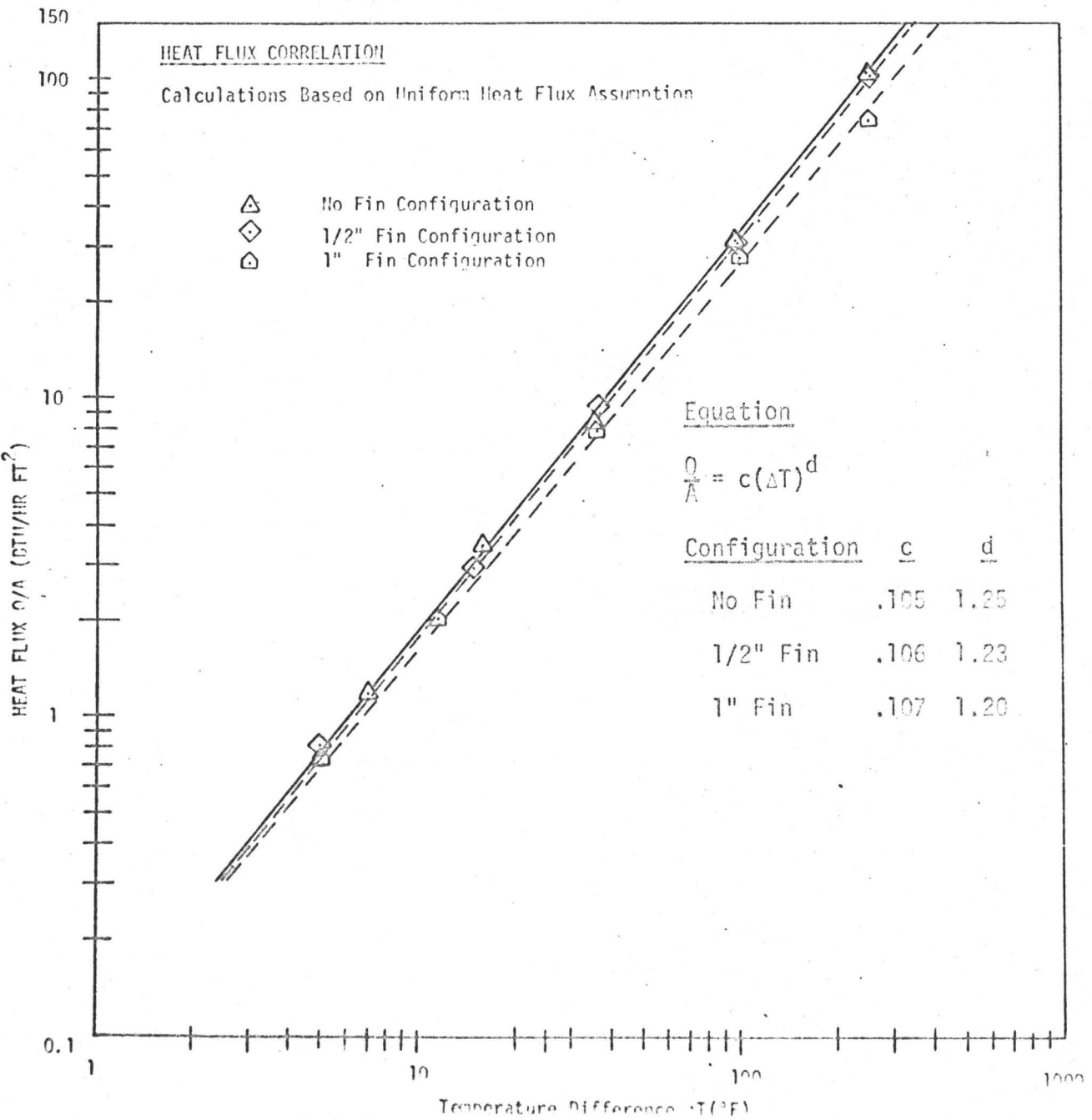


Figure #19

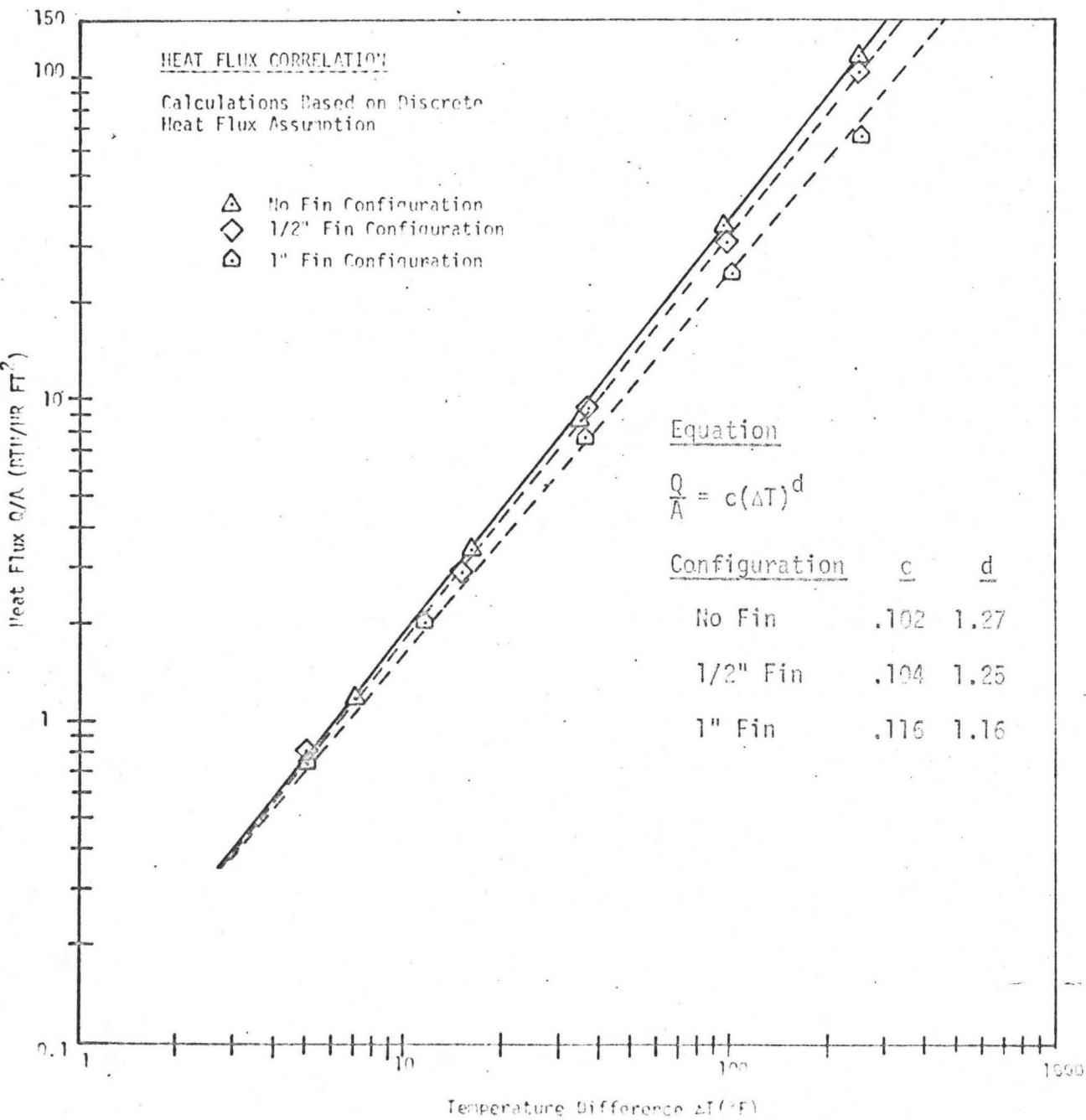


Figure #20

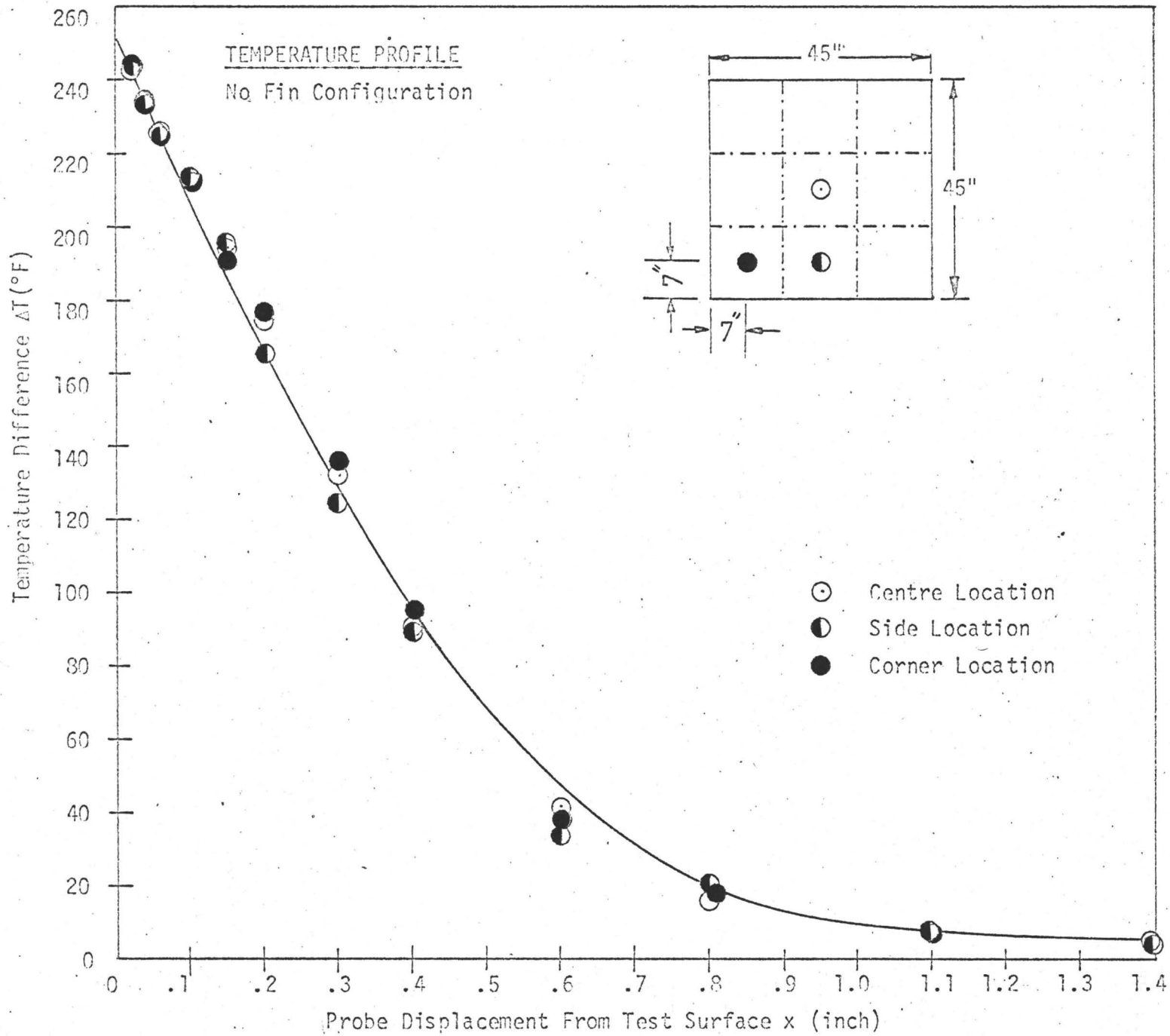


Figure 21

SCHLIEREN PHOTOGRAPHS

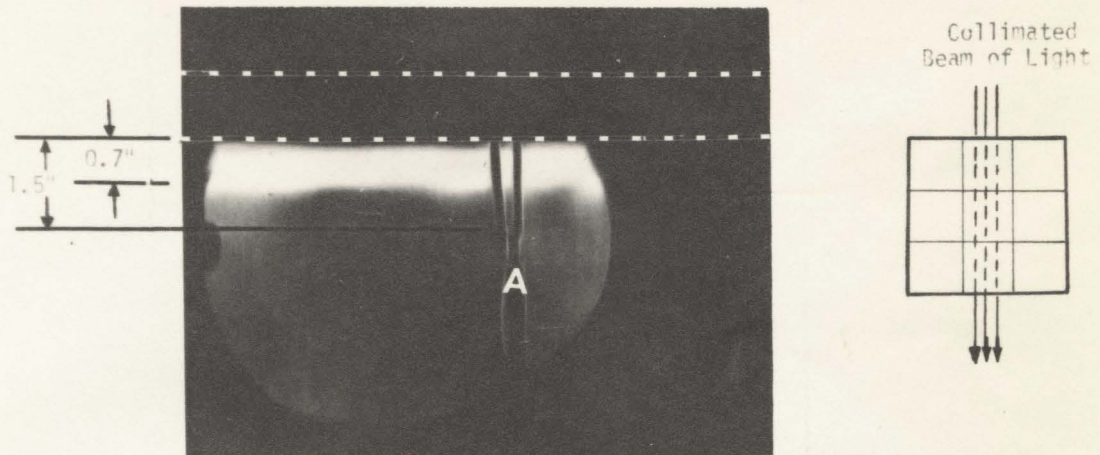


FIGURE # 22

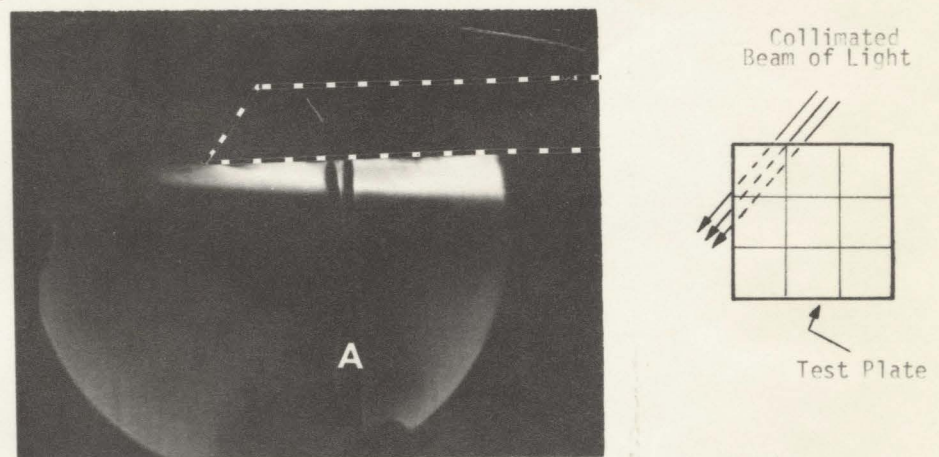


FIGURE # 23

----- Test Plate Boundary
 A Thermocouple Probe

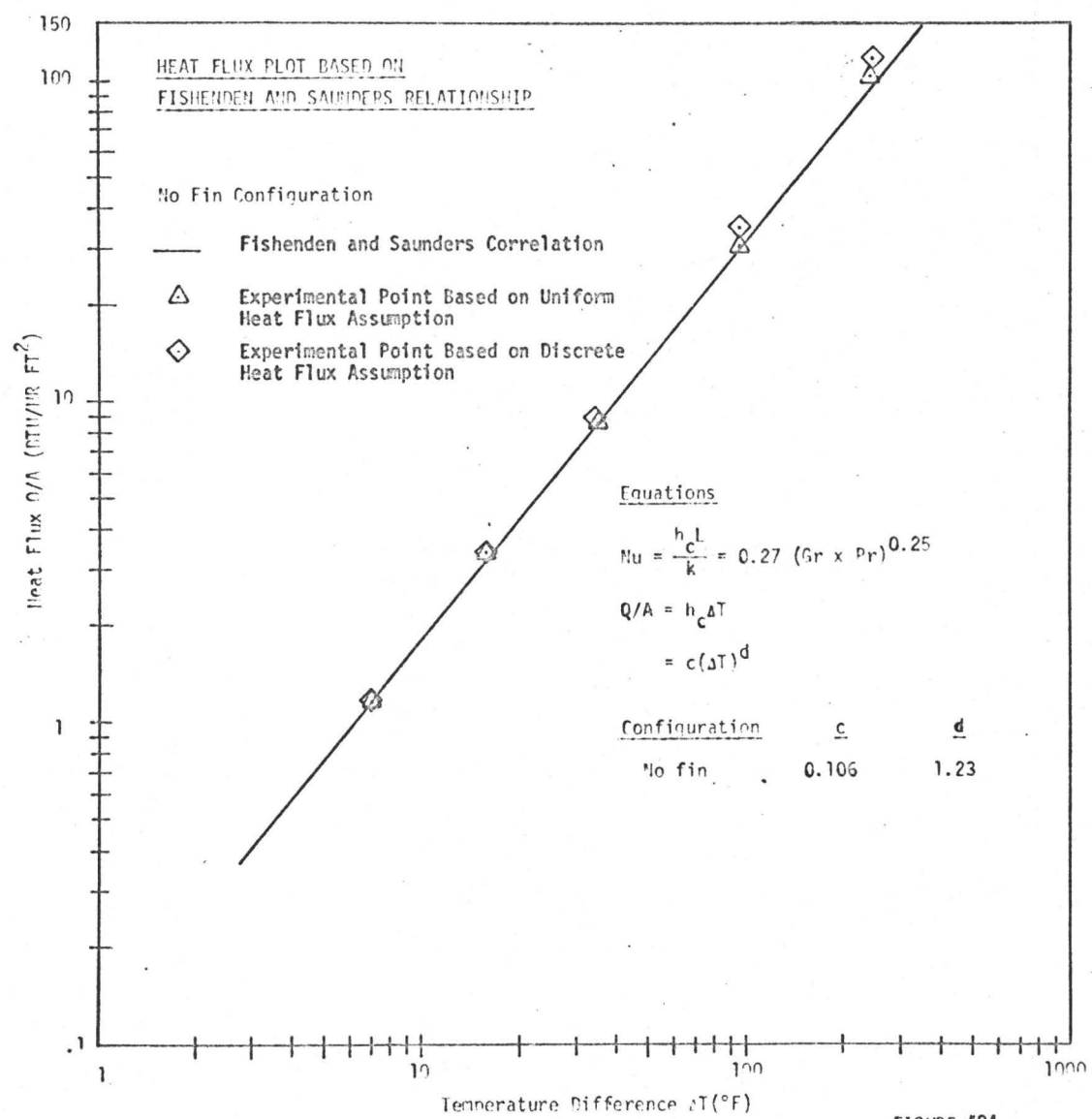
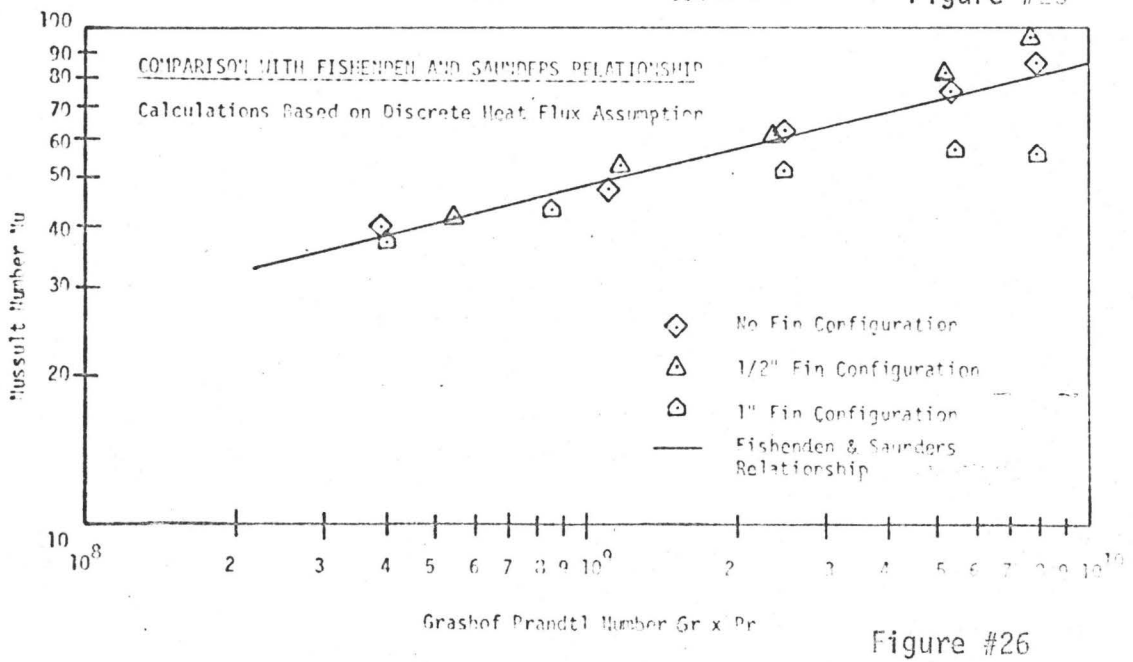
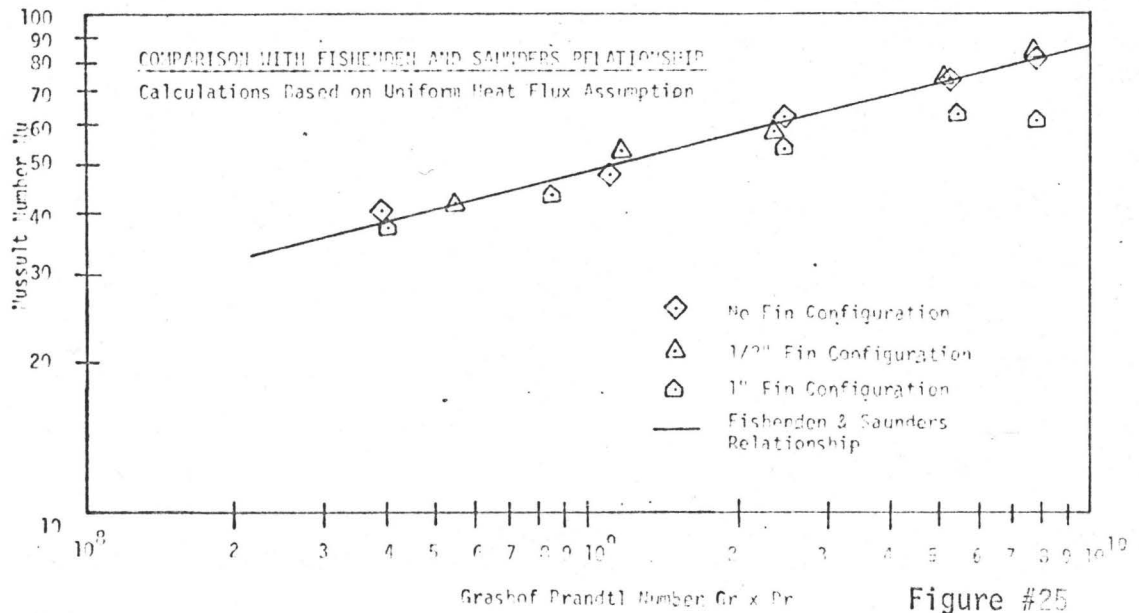


FIGURE #24



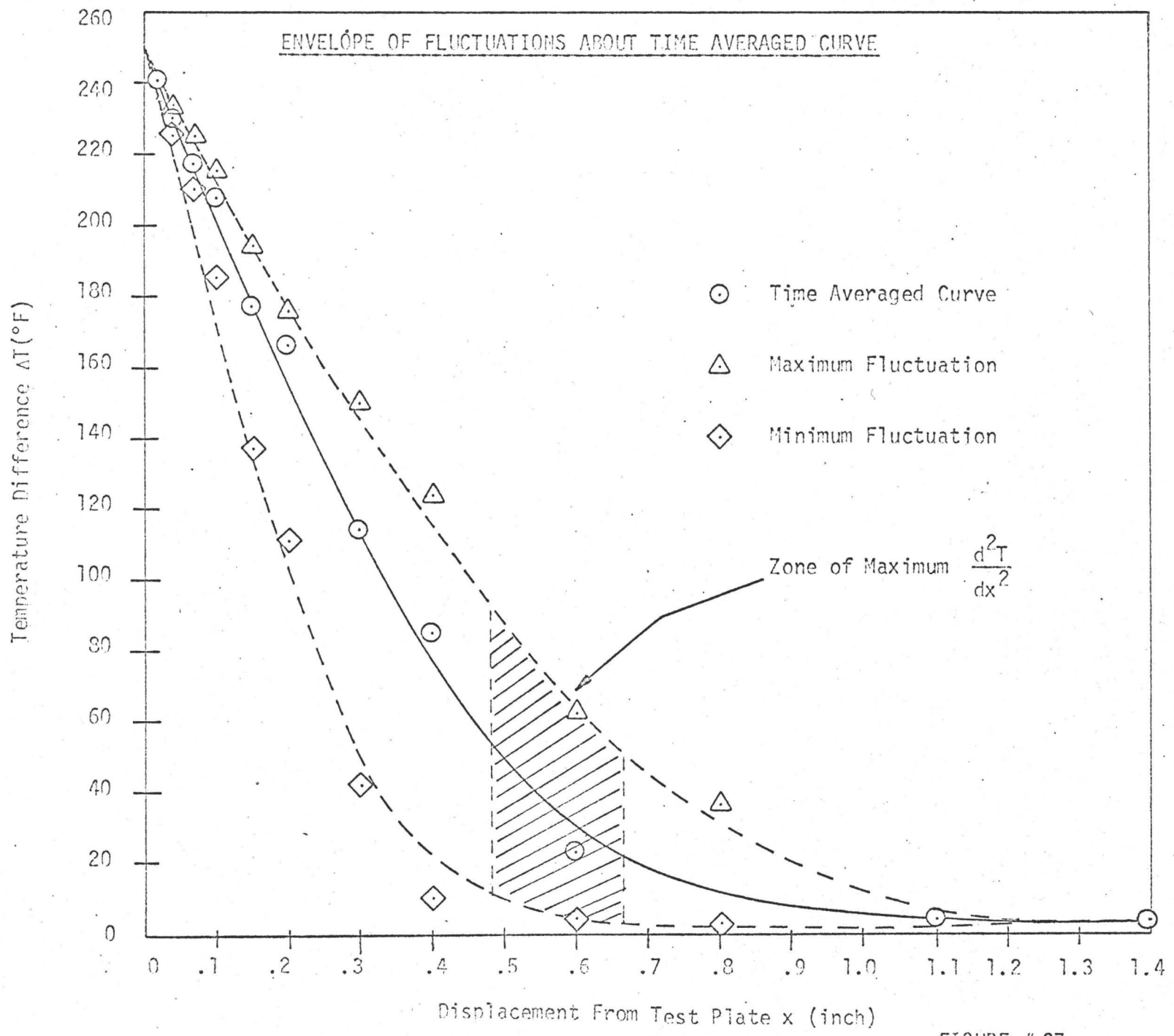


FIGURE # 27

APPENDIX A

This appendix presents the set of results obtained with various probes which were tried for the measurement of temperature distribution in the air below the plate.

Figure (28) presents plots of ΔT versus x for three different probes. The results can be summarized in the following table.

TABLE II
Comparison Of Various Probes

Probe #	Extrapolated $\Delta T(^{\circ}F)$	Actual * $\Delta T(^{\circ}F)$	Discrepancy ($^{\circ}F$)	Remarks
I	246	247	1	Acceptable
II	194	235	41	Not Acceptable
III	140	195	55	Not Acceptable

* Actual Temperature is obtained by subtracting T_{∞} from T_s measured with embedded thermocouples.

TEMPERATURE PROFILES OBTAINED WITH VARIOUS PROBES

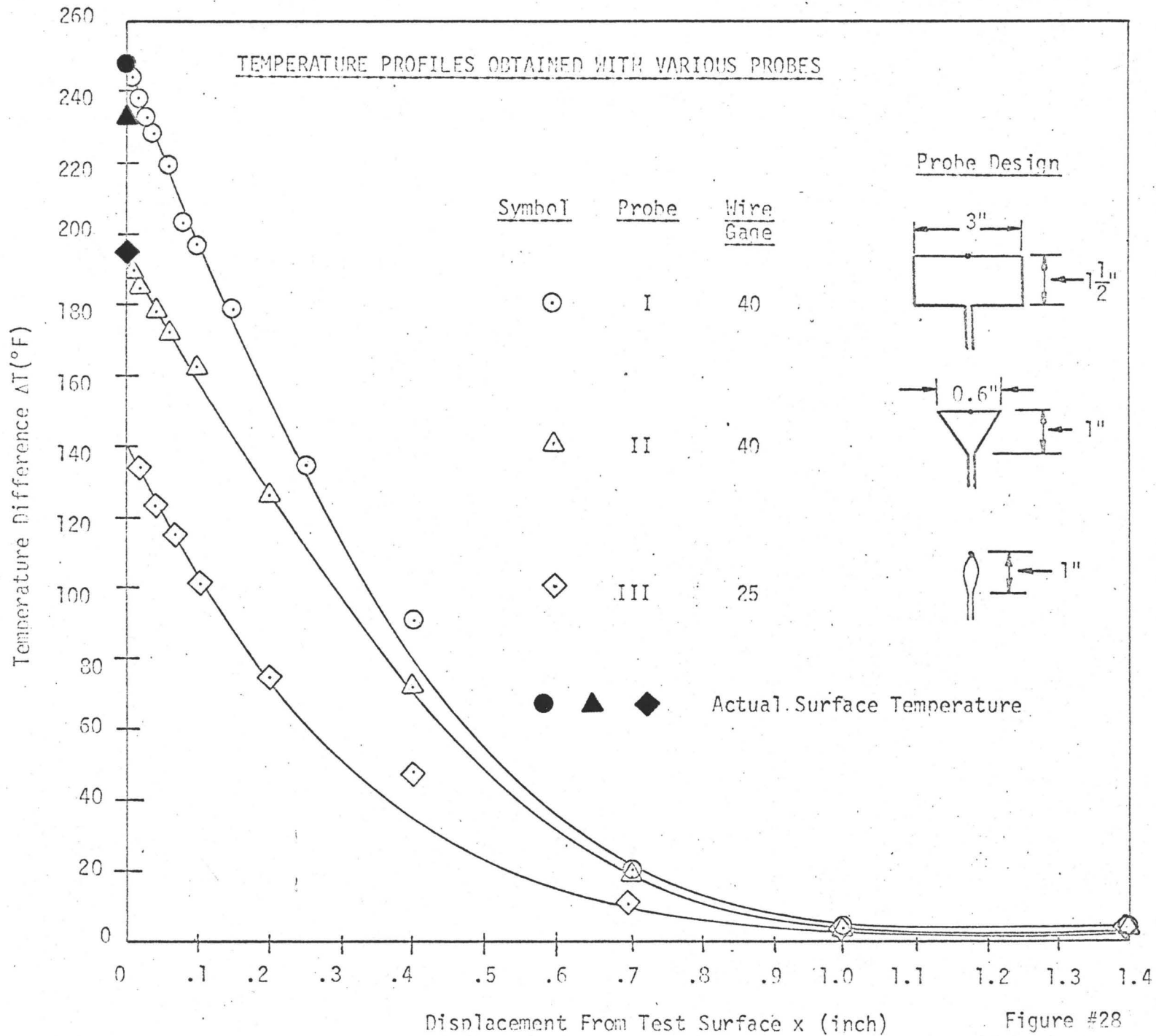


Figure #28

APPENDIX B

This appendix presents the energy balance performed on the system comprised of the present experimental set up for two tests pertinent to the plate without edge strips.

Various parameters pertinent to the calculations are as follows:

	<u>Test I</u>	<u>Test II</u>
Plate Surface Temperature, T_s :	330°F	177°F
Insulation Cover Temperature, T_c :	104°F	86°F
Ambient Temperature, T_∞ :	80°F	80°F
Length of the Plate, L :		3.75 ft.
Length of the Cover, L_c :		3.67 ft.
Height of the Cover, L_H :		0.52 ft.
Height of Bevelled Edges, L_E :		0.083 ft.

Calculations for the energy losses based on above information is as follows:

<u>Free Convection Losses</u>	<u>Test I</u>	<u>Test II</u>
(A) <u>Insulation Top Cover:</u>		
Film Temperature		
$T_f = (T_c + T_\infty)/2$	92°F	83°F
$\Delta T = T_c - T_\infty$	24°F	6°F
$Gr \times Pr = \left(\frac{\rho \beta g L_c^3}{\mu^2}\right) \cdot \Delta T \cdot L_c$		
(Properties Evaluated At T_f)	2.3×10^9	6.35×10^8

For Heated Plate Facing Upward:

$$Nu = \frac{h_c L_c}{k} = 0.14 (GrPr)^{1/3}$$

[Reference (12)]

$$h_c = \frac{Nu \cdot k}{L_c}$$

$$\text{Heat Flux} = h_c (T_c - T_\infty)$$

Test I

185

Test II

120

$$0.775 \frac{\text{Btu}}{\text{hrft}^2 \text{F}} \quad 0.496 \frac{\text{Btu}}{\text{hrft}^2 \text{F}}$$

$$18.6 \frac{\text{Btu}}{\text{hrft}^2} \quad 2.98 \frac{\text{Btu}}{\text{hrft}^2}$$

(B) Insulation Sides:

Average Temperature of Sides:

$$T_{is} = (T_c + T_s)/2$$

217°F

132°F

Film Temperature

$$T_f = (T_{is} + T_\infty)/2$$

149°F

106°F

$$\Delta T = T_{is} - T_\infty$$

137°F

52°F

$$Gr \times Pr = \left(\frac{\rho \beta g L_H^3}{\mu} \right) \Delta T \cdot L_H$$

(Properties evaluated at T_f)

2.52×10^7

1.25×10^7

For Heated Vertical Plates:

[Reference (12)]

$$Nu = \frac{h_c L_H}{k} = 0.48 (GrPr)^{1/4}$$

34.1

28.5

$$h_c = \frac{Nu \cdot k}{L_H}$$

$$1.095 \frac{\text{Btu}}{\text{hr ft}^2 \text{F}}$$

$$.856 \frac{\text{Btu}}{\text{hr ft}^2 \text{F}}$$

$$\text{Heat Flux} = h_c \Delta T$$

$$150 \frac{\text{Btu}}{\text{hrft}^2}$$

$$44.5 \frac{\text{Btu}}{\text{hrft}^2}$$

(C) Bevelled Edges:

	Test I	Test II
Film Temperature	205°F	128.5°F
ΔT	250°F	97°F
$GrPr = \left(\frac{g\beta\Delta T L_E^3}{\nu^2}\right) \Delta T \cdot L_E$	11.9×10^4	8.4×10^4
$Nu = 0.48 (GrPr)^{1/4}$ *	0.892	0.82
$h_c = \frac{Nu k}{L_E}$	$0.192 \frac{Btu}{hrft^2 F}$	$0.16 \frac{Btu}{hrft^2 F}$
Heat Flux	$48 \frac{Btu}{hrft^2}$	$18 \frac{Btu}{hrft^2}$

Radiation Losses

Assuming the plate to be a grey body in black surroundings, the following relationships can be written

$$F_{12} = \epsilon_1 \quad [\text{Reference (12)}]$$

where F_{12} = Grey body shape factor

ϵ_1 = Emmissivity of surface

The radiation heat transfer coefficient is defined as follows:

$$h_r = F_{12} F_T$$

$$0.172 \left[\left(\frac{T_1}{100}\right)^4 - \left(\frac{T_2}{100}\right)^4 \right]$$

where $F_T = \frac{0.172 \left[\left(\frac{T_1}{100}\right)^4 - \left(\frac{T_2}{100}\right)^4 \right]}{T_1 - T_2} \quad [\text{Reference (12)}]$

where T_1 = Temperature of emitting surface in ° Rankine

T_2 = Temperature of absorbing surface in ° Rankine

* Calculations are done on vertical plate basis though the edges are at 60° angle.

The values of F_T for given temperatures of T_1 and T_2 can be estimated from the chart in Reference (12).

The losses computed with the above formula using $\epsilon_1 = 0.1$ for dirty aluminum are as follows:

	<u>Test I</u>	<u>Test II</u>
(A) <u>Bottom Surface and Bevelled Edges:</u>		
Emmitting Temperature T_1	330°F	177°F
Absorbing Temperature T_2	80°F	80°F
From Chart, F_T	2.1	1.4
$h_r = \epsilon_1 F_T$.21 $\frac{\text{Btu}}{\text{hrft}^2\text{F}}$.14 $\frac{\text{Btu}}{\text{hrft}^2\text{F}}$
Heat Flux = $h_r \Delta T$	52.5 Btu/hrft ²	13.6 Btu/hrft ²
(B) <u>Insulation Top Cover:</u>		
Emmitting Temperature T_1	104°F	86°F
Absorbing Temperature T_2	80°F	80°F
From Chart, F_T	1.3	1.2
$h_r = \epsilon_1 F_T$	0.13 $\frac{\text{Btu}}{\text{hrft}^2\text{F}}$	0.12 $\frac{\text{Btu}}{\text{hrft}^2\text{F}}$
Heat Flux = $h_r \Delta T$	3.1 Btu/hrft ²	0.7 Btu/hrft ²
(C) <u>Insulation Sides:</u>		
Emmitting Temperature T_1	217°F	132°F
Absorbing Temperature T_2	80°F	80°F
From Chart, F_T	1.6	1.2
$h_r = \epsilon_1 F_T$	0.16 $\frac{\text{Btu}}{\text{hrft}^2\text{F}}$	0.12 $\frac{\text{Btu}}{\text{hrft}^2\text{F}}$
Heat Flux = $h_r \Delta T$	22.0 Btu/hrft ²	6.2 Btu/hrft ²

Total Energy Balance:

Area of Bottom Surface, A_S	14.1 ft ²
Area of Top Insulation Cover, A_C	13.3 ft ²
Area of Insulation Sides A_S	7.6 ft ²
Area of Bevelled Edges, A_E	1.2 ft ²

<u>Total Energy Supplied:</u>	1270 watts	370 watts
or	4340 Btu/hr	1265 Btu/hr

<u>Total Energy Losses:</u>	Btu/hr	Btu/hr
(A) Bottom Surface		
(i) Convection	1615.0 *	494.0 *
(ii) Radiation	740.0	192.0
(B) Insulation Top Cover		
(i) Convection	248.0	40.0
(ii) Radiation	42.0	10.0
(C) Insulation Sides		
(i) Convection	1143.0	340.0
(ii) Radiation	168.0	48.0
(D) Bevelled Edges		
(i) Convection	58.0	22.0
(ii) Radiation	63.0	16.0
TOTAL	<u>4032.0</u>	<u>1162.0</u>
Discrepancy:	6.0%	8.0%

* As measured by present experimental study.